Aksu *et al. Geothermal Energy* (2025) 13:37
https://doi.org/10.1186/s40517-025-00361-6

Geothermal Energy

RESEARCH Open Access

3D structural controls of a high-enthalpy geothermal field in an extensional setting: the Kizildere geothermal field (Western Türkiye)

Baykan Aksu[1], Bora Uzel[2] and Nuretdin Kaymakci[1,3*]

*Correspondence:
Kaymakci@metu.edu.tr

[1] Department of Geological Engineering, Middle East Technical University, 06531 Ankara, Türkiye
[2] Department of Geological Engineering, Dokuz Eylül University, 35160 İzmir, Türkiye
[3] Department of Neotectonics and Thermochronology Institute of Rock Structure and Mechanics of the Czech Academy of Science V Holesovickach, 94/41 182 09, Prague 8, Czech Republic

Abstract

The Kızıldere Geothermal Field (KGF), situated at the eastern margin of the Büyük Menderes Graben, is the most productive high-enthalpy geothermal system in Türkiye, with reservoir temperatures exceeding 240 °C and an installed capacity of over 360 MW. Its heat is derived from crustal thinning, shallow Curie depths, and lithospheric extension related to the post-Oligocene evolution of the Menderes Metamorphic Core Complex. This extensional tectonic setting produces high regional heat flow (up to 120 mW/m^2) and steep geothermal gradients that favour deep fluid circulation. To resolve the structural and hydrogeological controls on this system, we combined detailed field mapping, paleostress and kinematic analyses, 76 boreholes (530–3882 m), and 3D geological and thermal modelling. The results reveal that fault architecture is the principal control on fluid flow and geothermal productivity. E–W-striking high-angle normal faults act as major recharge pathways for meteoric waters, whereas NE-trending sub-vertical transfer faults, particularly the Gebeler Fault, form vertical conduits that enable the rapid ascent of thermal fluids. Intersections of these faults create favourable zones, where fractured marbles, quartzites, and carbonate-rich basin-fill units function as reservoirs, sealed by gneisses, schists, and clay-rich Miocene deposits. This study demonstrates that the interplay between fault geometry and lithology governs the exceptional productivity of the KGF. The insights gained provide a predictive framework for targeting high-permeability zones, extensional geothermal systems in Western Anatolia, and similar tectonic settings worldwide.

Highlights

- The Kızıldere Geothermal Field (KGF) in Western Anatolia, a high-enthalpy extensional domain-type, is controlled by complex fault patterns.
- 3D geological modelling, using field and borehole and seismic data, reveals the structural control on geothermal fluid percolation.
- Transfer faults, enhance permeability and fluid circulation, providing sweet spots for geothermal exploitation.

Keywords: Kızıldere geothermal field, Extensional tectonics, Western Anatolia, Transfer faults, 3D modelling, Geothermal exploration

Springer Open

© The Author(s) 2025. **Open Access** This article is licensed under a Creative Commons Attribution 4.0 International License, which permits use, sharing, adaptation, distribution and reproduction in any medium or format, as long as you give appropriate credit to the original author(s) and the source, provide a link to the Creative Commons licence, and indicate if changes were made. The images or other third party material in this article are included in the article's Creative Commons licence, unless indicated otherwise in a credit line to the material. If material is not included in the article's Creative Commons licence and your intended use is not permitted by statutory regulation or exceeds the permitted use, you will need to obtain permission directly from the copyright holder. To view a copy of this licence, visit http://creativecommons.org/licenses/by/4.0/.

Introduction

Geothermal energy is a critical renewable resource offering sustainable and low-emission electricity generation. Globally, approximately 92 billion kWh of electricity is produced annually from geothermal sources across 27 countries. Türkiye ranks among the leading geothermal energy producers, primarily due to its tectonically active setting, which hosts numerous high-enthalpy geothermal systems. The development of a geothermal system requires several essential components: a tectonically active region facilitating heat transport; a heat source, either magmatic or derived from deep crustal processes such as extension and thinning; a reservoir consisting of porous and permeable rocks; an impermeable caprock maintaining reservoir pressure; and a fluid source, generally meteoric in origin or hydrothermal in circulation (Dickson and Fanelli 2018; Moeck 2014; Gudmundsson 2022; Khodayar and Björnsson 2024).

The Kızıldere Geothermal Field (KGF), one of the most productive high-enthalpy fields in Türkiye, is situated within the Büyük Menderes Graben—an extensional basin developed as part of the Aegean–Western Anatolian Extensional System. Structurally, the field is controlled by a complex fault network, including low-angle detachment faults, NE-striking sub-vertical transtensional faults, and E–W trending high-angle normal faults with listric geometries (Gessner et al. 2001; Thomson and Ring 2006) (Fig. 1b). Transfer faults, which link normal fault segments, play a particularly important role at KGF by enhancing fracture permeability, promoting fluid circulation, and contributing to stress field rotation and fault dilation (Homberg et al. 2010). These structures create vertically extensive fluid pathways that connect deep geothermal reservoirs to the surface.

The geothermal potential of Western Anatolia, including the Kızıldere Geothermal Field (KGF), is fundamentally linked to its post-collisional extensional tectonic evolution. The region forms part of a broader Aegean geodynamic system characterized by crustal thinning and asthenosphere upwelling, which collectively generate elevated regional heat flow. Measured heat flow values range from 70 to 140 mW/m^2 across the Menderes Massif, reaching approximately 120 mW/m^2 near the KGF (Erkan 2015; Balkan-Pazvantoğlu 2021).

Unlike magmatic geothermal provinces, Western Anatolia lacks significant shallow intrusions, except for the Kula volcanic field, which is about 70 km north of KGF. Instead, its thermal regime is controlled by lithospheric extension associated with the post-Oligocene evolution of the Menderes Metamorphic Core Complex (MCC) (Bozkurt 2001; Bozkurt and Oberhänsli 2001; Gessner et al. 2001; Ring et al. 2003; Kaymakci 2006; Kaymakci et al. 2018; Roche et al. 2018). This extensional evolution dissected the MCC into multiple tectonic domains, bounded by high-angle normal faults that act as primary conduits for deep fluid circulation (van Heiningen and Kaymakci 2024). The Aegean domain, in particular, exhibits steep geothermal gradients where heat transport is strongly controlled by fault architecture (Erkan 2014, 2015; Jolivet et al. 2021).

Geophysical observations further support the extensional origin of the geothermal regime. Crustal thickness in western Anatolia is approximately 26 ± 2 km near 32°E longitude and decreases westward (Karabulut et al. 2019; Vanacore et al. 2013; Tezel et al. 2013). Curie point depths are similarly shallow, reaching 9 ± 2 km in the Denizli–KGF region (Dolmaz et al. 2005; Şalk et al. 2005), comparable to highly extended or volcanic

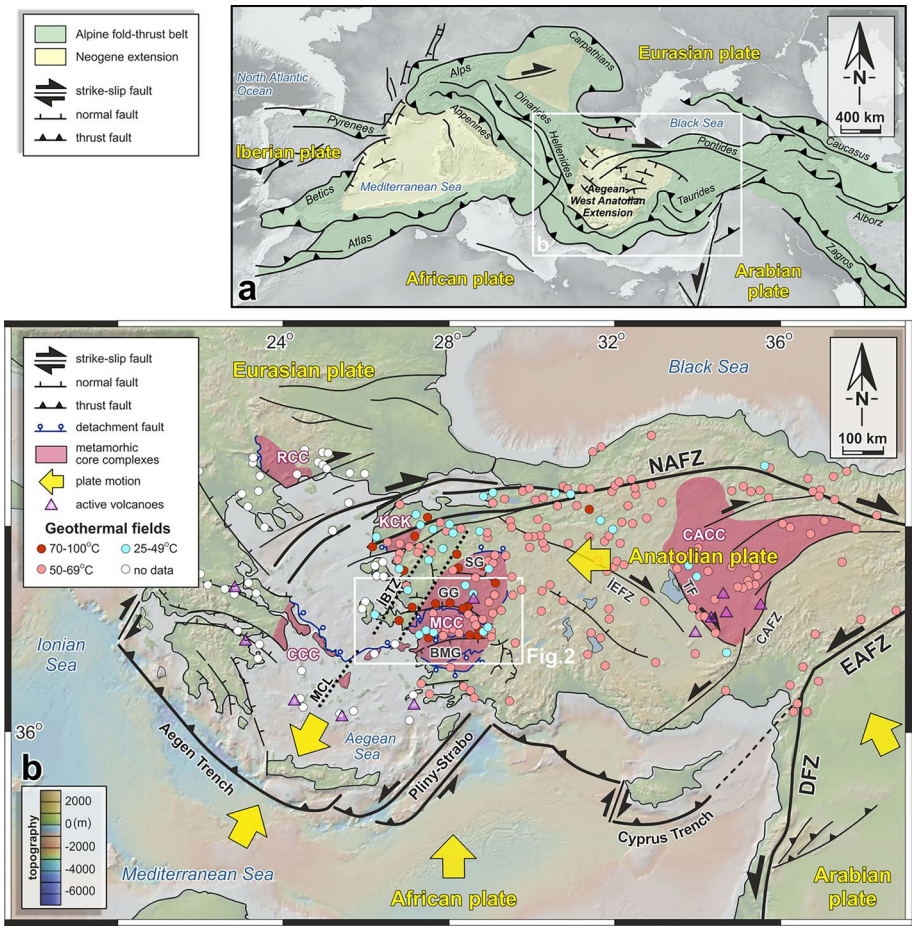


Fig. 1 **a** Tectonic map of the Mediterranean region showing the Alpine fold-thrust belt (green) and the distribution of the main back-arc extensional areas (yellow) within (modified from Jolivet et al. 2021). **b** Simplified tectonic map of the Anatolian Plate showing the major structural elements and geothermal fields (Bozkurt 2001; Uzel et al. 2013; Emre et al. 2018; Roche et al. 2018; Jolivet et al. 2021). Please note the increase in the number of geothermal areas and their high temperatures in Western Anatolia. *NAFZ* North Anatolian Fault Zone, *EAFZ* East Anatolian Fault Zone, *DSF* Dead Sea Fault, *CAFZ* Central Anatolian Fault Zone, *TF* Tuzgölü Fault, *İEFZ* İnegöl-Eskişehir Fault Zone, *İBTZ* İzmir-Balıkesir Transfer Zone, *MCL* Mid-Cycladic Lineament, *SG* Simav Graben, *GG* Gediz Graben, *KMG* Küçük Menderes Graben, *BMG* Büyük Menderes Graben, *MCC* Menderes Core Complex, *CCC* Cycladic Core Complex, *RCC* Rhodope Core Complex, *CACC* Central Anatolian Crystalline Complex

terrains. These factors—crustal thinning, shallow Curie depths, and E–W-trending graben systems—collectively account for the high regional heat flow and favourable geothermal conditions that underpin the productivity of the KGF.

Operationally, the KGF has undergone substantial development since the installation of the first 15 MW power plant in 1984 by the Turkish Electricity Authority. After the field's transfer to Zorlu Energy in 2008, intensive exploration and development increased its capacity significantly. At present, three power plants with a total capacity of 260 MW are operated by Zorlu Energy, while six additional plants totalling 106 MW are managed by Greeneco Energy (TEİAŞ, 2020). Ongoing development continues to position KGF as one of the most productive geothermal fields globally.

Despite this success, the specific geological structures, fault networks, and lithological factors controlling fluid flow and reservoir permeability at KGF remain poorly constrained and not fully understood. This study aims to characterize the structural framework that governs fluid migration, with particular emphasis on the role of both normal and transfer faults in creating and maintaining high-permeability pathways. Although the influence of these fault systems is widely accepted in extensional geothermal settings, direct evidence from KGF remains limited. To address this, a combination of field-based structural analysis, borehole data, and seismic sections was used to construct a high-resolution 3D geological model. The constructed model is used to identify and evaluate reservoir and caprock distributions that govern fluid storage and confinement.

The study encompasses detailed field mapping of faults and stratigraphic units, paleostress and fault kinematic analyses, 3D subsurface modelling based on 76 borehole data with depth ranges changing between 530 and 3882 m and confidential seismic sections, and evaluation of the structural–hydrogeological interactions that create favourable permeability zones within the geothermal system.

The findings of this study contribute to the broader understanding of geothermal dynamics in extensional domain-type systems, where permeability and fluid transport are predominantly governed by fault zone architecture. By identifying key structural controls, the study provides a framework for optimizing geothermal exploration and development strategies in similar tectonic settings.

Background

In western Türkiye, geothermal systems are predominantly associated with an extensional tectonic regime related to the development of Menderes Core Complex (MCC) by the end of Oligocene–Early Miocene (Bozkurt 2001; Bozkurt and Oberhansli 2001; Ring et al. 2003; Gessner et al. 2001; Thomson and Ring 2006; Kaymakci et al. 2018; Uzel et al. 2020; Gülyüz et al. 2024) and younger dominantly E–W striking high-angle normal faults that dissected the MCC into three main tectonic domains (van Heiningen and Kaymakci 2024). The heat flow in the region reaches as high as 120 mW/m^2 in the region (Erkan 2015; Balkan-Pazvantoğlu et al. 2021). Lack of any magmatic body in the region implies that heat flow is primarily governed by crustal thinning and asthenosphere upwelling, resulting from regional extensional tectonics (Fig. 1; Hetzel et al. 1995; Bozkurt and Park 1994, Bozkurt 2001; Bozkurt and Oberhansli, 2001; Gessner et al. 2001; Ring et al. 2003; Thomson and Ring 2006; Kaymakci 2006; Alçiçek et al. 2018, 2016, 2013, 2019a, b; Roche et al. 2018; Sümer et al., 2020; Brogi et al. 2021).

The Aegean domain exhibits some of the highest geothermal gradients in Türkiye, with heat transport largely controlled by fault-related structures (Erkan 2014, 2015; Roche et al. 2018; Jolivet et al. 2021). In extensional settings, normal faults serve as primary conduits for deep fluid circulation and act as key permeability pathways (Meixner et al. 2016; Gudmundsson 2022). In recent years, increasing attention has been given to the role of transfer faults—strike-slip or oblique-slip structures that accommodate differential extension between normal fault segments. These faults significantly enhance permeability by generating interconnected fracture networks and facilitating vertical and lateral fluid migration. Moreover, they can function as structural traps that localize

geothermal reservoirs and influence the spatial variability of high-permeability zones (Roche et al. 2018; Liotta et al. 2020, 2021; Gudmundsson 2022; Brogi et al. 2023).

Methods

This study integrates field investigations, borehole data, and 3D geological modelling, combining mapping, fault analysis, stratigraphy, geothermal feature documentation, to characterize the area's structural framework and geothermal potential.

Geological mapping was conducted to define lithological units, delineate major structural features, and characterize the tectonic framework of the region. Special emphasis was placed on identifying fault systems and assessing their spatial relationships with stratigraphic units and geothermal manifestations. Faults were systematically mapped, and their geometries and kinematic indicators, such as slickensides and slickenfibers showing the sense of movement, were documented in the field. The recorded fault-slip data were analysed using Win-Tensor Software (Delvaux and Sperner 2003) to reconstruct the regional paleostress history. The stratigraphic framework and lateral continuity of lithological units were delineated using 1:25,000 scale topographic maps, which served as a basis for refining subsurface fault geometries and understanding their role in geothermal fluid migration.

In addition to structural mapping, geothermal surface manifestations such as hot and cold springs, fumaroles and gas seeps were also documented as indicators of deep-seated geothermal activity. To complement field observations, borehole data were incorporated to provide additional constraints on the lithological, structural, and thermal characteristics of the subsurface. Borehole information, including petrographic descriptions, mud loss records, and static temperature measurements, was analysed in conjunction with surface data to refine the interpretation of geothermal reservoir properties and fluid flow pathways.

All collected field and borehole data were integrated into a three-dimensional geological modelling workflow using Seequent Leapfrog Geo Software. The modelling process involved constructing lithological models representing the spatial distribution of rock units, developing structural models that incorporated mapped faults and inferred subsurface geometries, and generating thermal models integrating borehole temperature data and inferred heat flow patterns. The resulting 3D geological and thermal models were subsequently validated against confidential 2D seismic sections to ensure internal consistency and accuracy in fault geometries and stratigraphic correlations. This integrated approach provides a robust framework for understanding the structural controls on geothermal systems in the study area, facilitating the assessment and development of geothermal energy resources.

Geological settings

Stratigraphy of the KGF

The major rock units in the study area from oldest to youngest comprise Palaeozoic–Mesozoic metamorphic rocks of the Menderes Massif, Miocene Basin infill including Kızılburun, Sazak, Kolankaya, and Tosunlar formations, and Quaternary Alluvium (Figs. 3 and 4; Şimşek 1984; Alçiçek et al. 2007; Bozcu 2010).

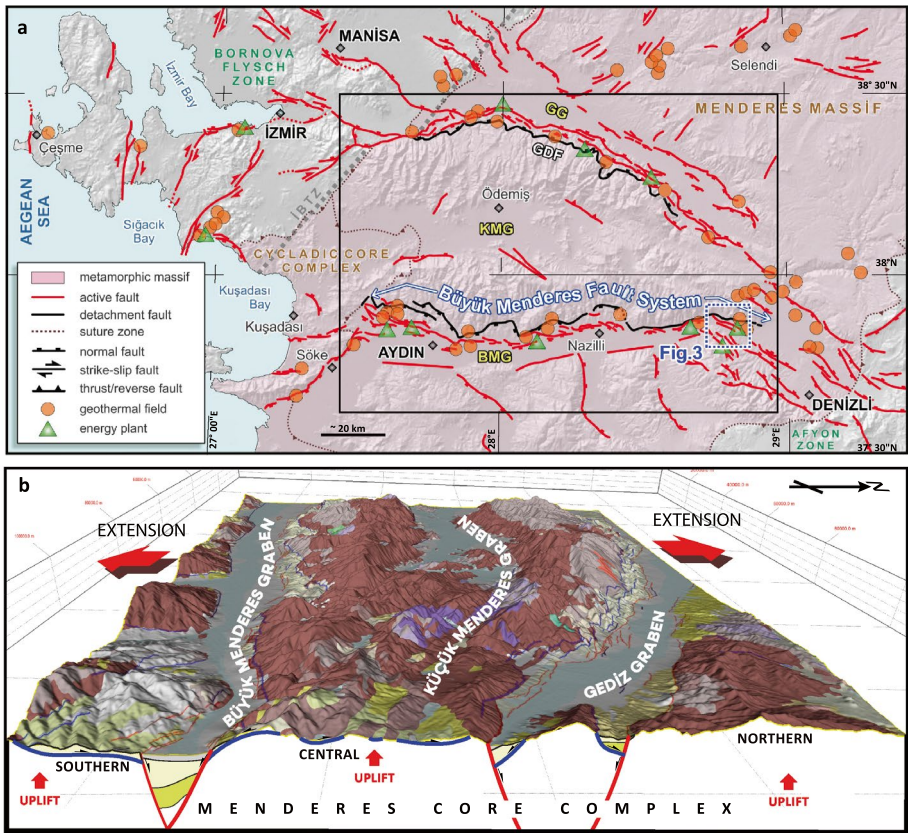


Fig. 2 **a** Active fault map of the Büyük Menderes Graben and adjacent region (Uzel et al. 2013) and active faults (Emre et al. 2018) and distribution of the geothermal fields and energy plants (Şimşek 1984, 2003; Akkuş et al. 2005; Roche et al. 2018). Please note that the locations of the geothermal areas are aligned mostly along the E–W-trending graben-bounding normal faults. **b** 3D perspective view of the horst–graben system in Western Anatolia and a geological section showing the main structures in the region

Menderes massif

The Menderes Massif represents the largest tectonic unit in Western Anatolia. It is structurally overlain by ophiolitic rock assemblages derived from the İzmir–Ankara–Erzincan Suture Zone (Bozkurt and Oberhänsli 2001). Exposed within a tectonic window bounded by the Bornova Flysch Zone and the Afyon Zone (Fig. 2; Okay et al. 2012; Çetinkaplan et al. 2020), the Menderes Massif comprises two distinct metamorphic rock assemblages: a Pan-African gneissic core comprising augen gneiss, quartzite, metagranite, and other high-grade metamorphic lithologies, and overlying so-called cover rocks including Palaeozoic schists, which are unconformably overlain by Mesozoic to Eocene marbles belonging to passive margin sequences of the Neotethys Ocean (Bozkurt and Oberhänsli 2001, and references therein).

Within the study area and across the Büyük Menderes Graben, Pan-African rocks are predominantly observed as tectonic slices thrust over the lower-grade cover rocks. The cover sequence consists of a variety of low-grade metamorphic units, including schists, phyllites, quartzites, and marbles. The schists display compositional variability, comprising garnet-bearing micaschist, calc-schist, quartz-muscovite schist, and chlorite schist (Fig. 5a, b). Metacarbonate units occur either as thin schist–marble intercalations, a few metres in thickness, or as massive marble bodies exceeding 100 m in thickness

(Fig. 4). Due to its complex deformation history, both the core and cover rocks exhibit high porosity and permeability, making them favourable for geothermal fluid circulation. Brittle deformation is particularly well-developed in carbonate- and quartz-rich lithologies, further enhancing their reservoir potential.

Given these lithological and structural characteristics, the marbles of Menderes Massif are considered a highly suitable geothermal reservoir rock (designated as Reservoir 1 in Fig. 4). Consequently, many geothermal power plants in Western Anatolia, including those in Germencik, Nazilli, and Kızıldere (Fig. 2), are situated within this unit (Roche et al. 2019; Siefert et al. 2021).

Miocene basin infill

The Miocene sedimentary fill of the Büyük Menderes Graben consists of fluvial–lacustrine graben deposits that unconformably overlie the metamorphic basement of the Menderes Massif. These deposits have been subdivided into three distinct formations, including Kızılburun, Sazak, and Kolankaya (Sümer et al., 2020) (Fig. 4).

The Kızılburun Formation rests with an angular unconformity on the basement and has been dated to the Early Miocene–Early Middle Miocene (Alçiçek et al. 2007). In the study area, it is exposed within a narrow corridor bounded by the Gökdere and Büyük Menderes detachment faults on the northern flank of the graben (Fig. 3). The lower part of the formation is characterized by matrix-supported, unsorted, polygenetic conglomerates composed of boulders and blocks intercalated with mudstone and sandstone. The size of the clasts ranges from a few centimetres to several metres, gradually decreasing toward the upper levels, where the sequence transitions into sandstone and mudstone alternations. Sandstones are massive, medium- to coarse-grained, and poorly sorted, while mudstones are medium-bedded and intercalated with siltstone layers. The depositional environment of the lower Kızılburun Formation is interpreted as a high-energy, fault-controlled, proximal-to-mid alluvial fan system (Alçiçek et al. 2007). The upper part consists of massive mudstones, laminated siltstone–sandstone alternations, conglomerates, and thin limestone lenses interbedded with coal (Fig. 5c). The overall fining-upward nature of the succession, with a progressive decrease in grain size and bedding thickness, reflects a transition from proximal alluvial fan to more distal lacustrine settings. Our field observations indicate that the Kızılburun Formation is bounded to the west by the Pelitliada Fault (Fig. 3). The lateral and vertical continuity of impermeable mudstone layers within this unit plays a crucial role as a caprock overlying the fractured basement reservoir (Reservoir 2 in Fig. 4).

The Sazak Formation conformably overlies the Kızılburun Formation and has been dated to the Middle Miocene–Early Late Miocene (Alçiçek et al. 2007). Its lower section is composed of alternating marl, claystone, and clayey limestone. Marls are generally thin- to medium-bedded with parallel laminations, while clayey limestones are medium- to thick-bedded, occasionally fossiliferous. The claystone layers are thin-bedded, silty, and contain organic-rich horizons. The middle part of the Sazak Formation consists of massive limestone interbedded with sandstone layers. These limestones are generally thick-bedded to massive, exhibiting karstic features, partial dolomitization, and fossil content, including gastropods. Thin chert bands and gypsum-rich layers are also present (Fig. 5e, f). The increasing gypsum content toward

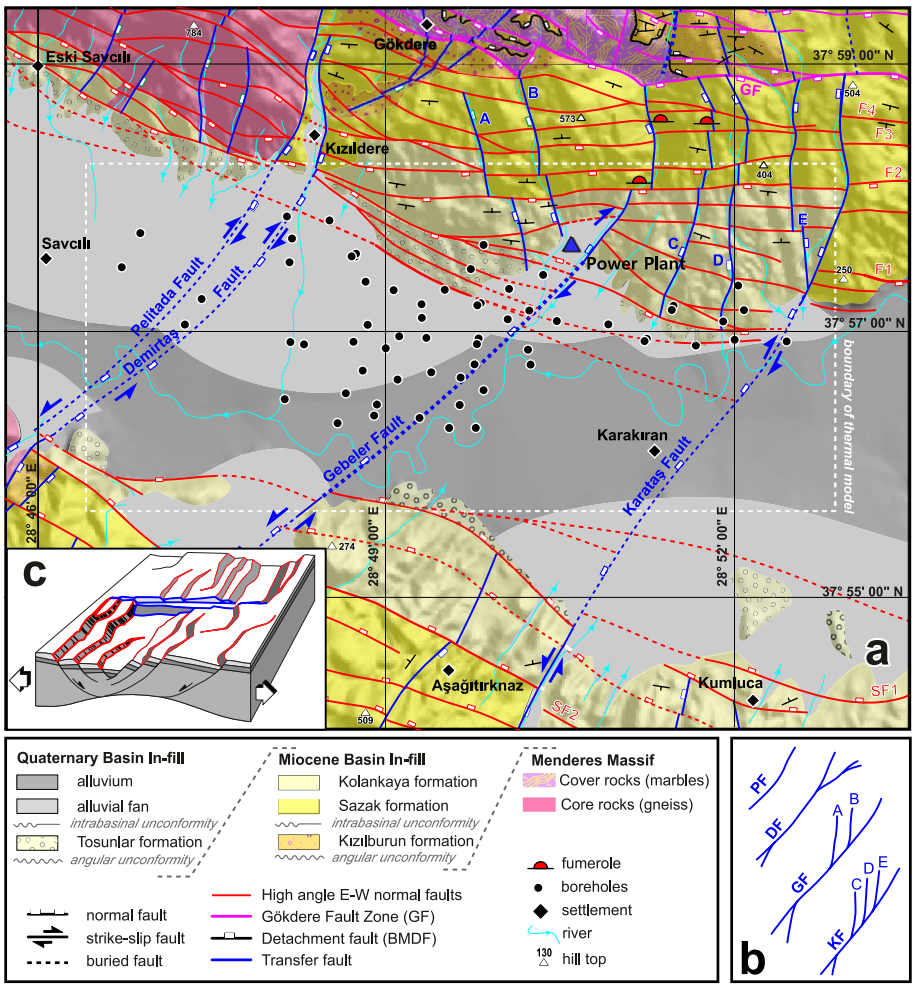


Fig. 3 **a** Geological map of the study area (after Sümer et al., 2020). **b** Simplified sketch view showing the segmentation of the NE-trending transfer faults. F1–F4 are segments of the Buharkent Fault. S1–S2 are the segments of the Sarayköy Fault. **c** Conceptual transfer fault geometry (adapted from Van der Pluijm and Marshak 2004). Please note the change in the relative displacement directions. *PF* Pelitada Fault, *DF* Demirtaş Fault, *GF* Gebeler Fault, *KF* Karataş Fault, *BMDF* Büyük Menderes detachment fault, *GF* Gökdere Fault

the upper levels suggests a shift toward more arid climatic conditions during deposition. Sandstone beds within this interval are medium-bedded, well-sorted, fine- to medium-grained, and lithified with carbonate cement. The uppermost section consists of clayey limestones and limy shales, with the latter being very thinly laminated and containing organic-rich intervals. The depositional setting of the lower Sazak Formation is interpreted as a deep lacustrine system, while the increasing anhydrite content and dominance of carbonate deposition in the upper levels indicate a transition into a low-energy, arid, and saline shallow-lacustrine environment. Similar to the Kızılburun Formation, the Sazak Formation is truncated to the west by the Pelitliada Fault (Fig. 3). The karstic nature and brittle rheology of the Sazak Formation make it an excellent geothermal reservoir (Reservoir 3 in Fig. 4), as evidenced by the presence of numerous hot springs and fumaroles associated with limestone exposures (Fig. 3).

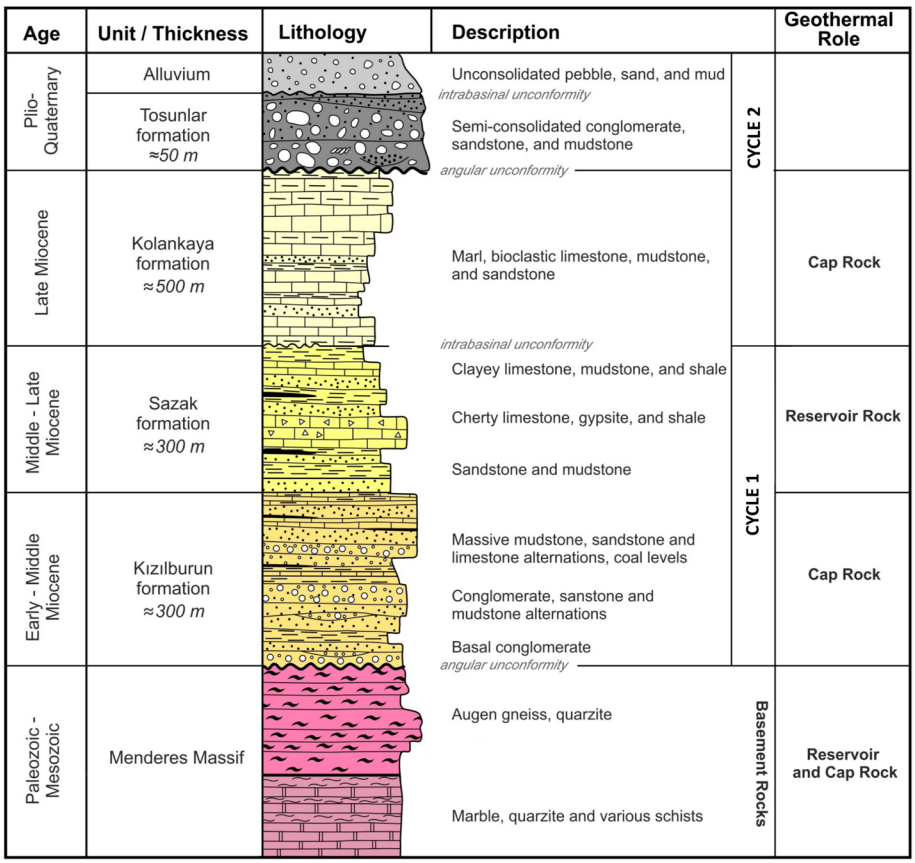


Fig. 4 Generalized tectonostratigraphic columnar section of the study area (after Alçiçek et al. 2007, 2015) and reservoir compartments of the Kızıldere Geothermal Field. *BMDF*: Büyük Menderes detachment fault

The Kolankaya Formation unconformably overlies both the basement rocks and the Sazak Formation (Fig. 4). It has been dated to the Middle–Late Miocene to Late Pliocene (Kaymakci 2006; Alçiçek et al. 2007). This formation is characterized by dominantly laminated, clay-rich marl interbedded with sandstone and bioclastic limestone. The marls are typically parallel-laminated to thick-bedded and include gypsum interlayers (Fig. 5e). Bioclastic limestones contain abundant fossil fragments cemented by carbonate (Fig. 5f). The prevalence of marl-dominated lithologies suggests deposition in a low-energy, brackish lacustrine environment (Alçiçek et al. 2007). Borehole data indicate that the formation has an average thickness of approximately 400 m, reaching up to 800 m in certain locations, though such thick exposures are not observed in the field. Subsurface data and field mapping indicate that the Kolankaya Formation extends beyond the Pelitliada Fault, covering the basement rocks around Eski Savcılı village, thereby postdating the fault (Fig. 3). The significant thickness, regional continuity, and impermeable nature of the marls make the Kolankaya Formation an effective caprock for the underlying geothermal reservoirs (Reservoir 4 in Fig. 4).

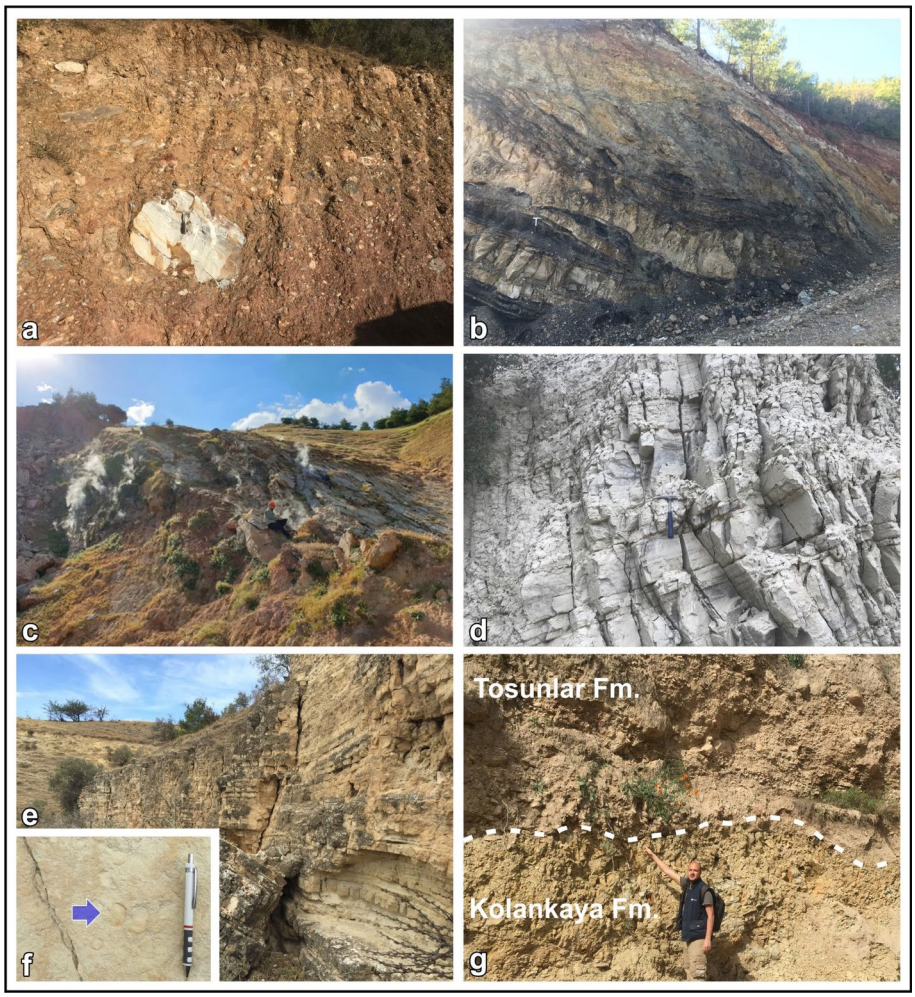


Fig. 5 Field photos of the Basement and Miocene Basin fill units. **a** A close-up view of Menderes Massif Neogene cover rocks near Gökdere Village. **b** A close-up view of Menderes Massif core rocks (gneisses) near Old Savcılı Village. **c** A field view of limestone–coal alternation of Kızılburun Formation at the north of the Gökdere Fault. **d** Cross-bedded clastics of the Sazak formation near Kızıldere Village. **e** General view of limestones of Sazak formation and **f** mollusk shells inside near Örenli Village. **g** Boundary between Kolonkaya and Tosunlar formations

Quaternary infill

The Quaternary sedimentary infill of the Büyük Menderes Graben has been subdivided into two primary units based on previous studies: the Tosunlar Formation and the alluvium (Sümer et al., 2020) (Fig. 4). These deposits unconformably overlie the older Miocene basin fill and represent the most recent phase of sedimentation within the graben system.

The Tosunlar Formation is characterized by a regional unconformity at its base (Fig. 5g) and has been assigned an Early Quaternary (Sarıca 2000; Kaymakci 2006). It consists predominantly of poorly sorted, polygenetic pebble- to boulder-sized conglomerates with occasional mudstone intercalations. Clast composition is primarily derived from pre-existing basement rocks and limestone fragments sourced from the older basin deposits. The grain size within this unit varies significantly, with clasts

ranging from pebbles to large boulders. The clasts are generally subrounded, suggesting a relatively high-energy depositional environment with limited transport distance. The formation exhibits weakly developed bedding, commonly with erosional bases, and is typically poorly consolidated, with a sandy matrix binding the larger clasts together.

Deposition of the Tosunlar Formation is interpreted as being controlled by fault activity, occurring in a high-energy debris-flow environment along the fronts of NE–SW and E–W trending normal faults (Fig. 3). The chaotic nature of deposition, poor sorting, and weak lithification result in relatively low porosity and permeability, making the Tosunlar Formation a poor-quality reservoir unit (Reservoir 5 in Fig. 4).

The remaining Quaternary basin fill is mapped as Alluvium, comprising unconsolidated and poorly sorted alluvial fan and fluvial deposits (Figs. 3 and 4). These sediments are dominated by loose sand, silt, gravel, and clay, representing recent depositional processes influenced by modern river systems and seasonal flood events. Due to their unconsolidated nature and high clay content in some areas, alluvial deposits do not exhibit significant reservoir potential and are not considered viable for geothermal fluid storage.

Structures of the KGF

As the pathways of hot geothermal fluids and cold meteoric waters, faults are one of the key components of an extensional domain-type geothermal system. Besides, faulting and brittle deformation can further enhance the reservoir quality of rocks by creating secondary porosity and permeability. Therefore, the faults in the KGF and its surroundings were carefully mapped and their kinematics were examined in detail. According to previous studies on the Büyük Menderes Graben (see Sümer et al., 2020 for details), our field observations and borehole data show that faults are divided into three categories: (1) Büyük Menderes detachment fault; (2) NE-trending transfer faults; (3) E–W trending high-angle normal faults (Fig. 3).

Büyük Menderes detachment fault

The Büyük Menderes detachment fault is a key structural feature in the geothermal system of Western Anatolia (Bozkurt and Oberhänsli 2001 and references therein). This low-angle normal fault (< 30° dip) with deep roots juxtaposes the Miocene basin-fill deposits with the underlying basement rocks. Exposed north of Gökdere (Fig. 3), the fault defines the boundary between the Menderes Massif and the Miocene deposits. Intense deformation has affected both the Miocene basin infill and the basement rocks, resulting in a complex fault zone, which is further displaced by E–W trending high-angle normal faults and their NE-trending transfer faults. This deformation zone is characterized by highly permeable features, such as brecciated, cataclastic, and calcite-cemented veins that facilitated fluid circulation. This fault zone is regarded as one of the most favourable targets for geothermal exploration since it separates marbles from the overlying sedimentary rocks dominated with immature sandstones and mudstones (Fig. 4).

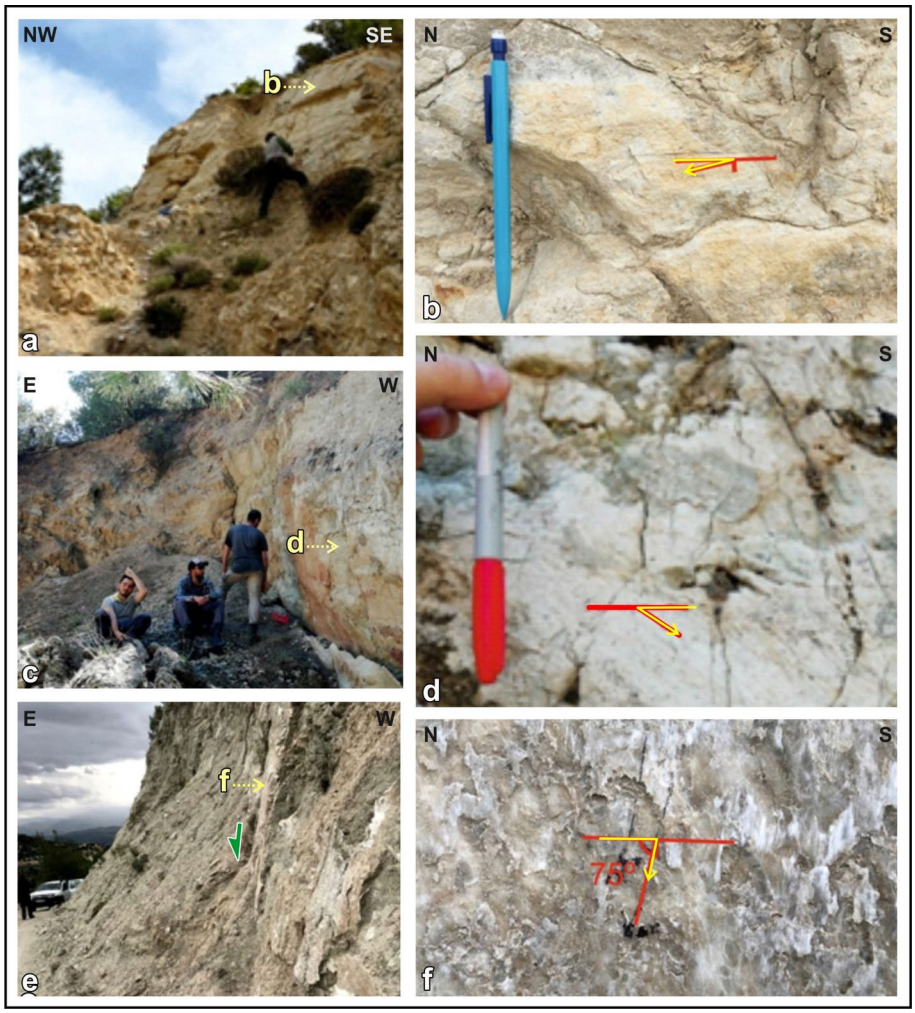


Fig. 6 Field views and kinematic data on the NE-trending transfer faults. **a** General view of the Karataş Fault, **b** a close-up view of slickenlines on the fault surface in Sütleğenli Valley. **c** General view of the Demirtaş Fault, and **d** a close-up view of slickenlines on the fault surface in Kavak Valley. **e** General view of the Pelitliada Fault, and **f** a close-up view of slickenlines on the fault surface in Kavak Valley

NE-trending transfer faults

These faults are primarily sub-vertical structures, orthogonal to the main E–W axis of the Büyük Menderes Graben and its basin-bounding faults (Fig. 3). We have mapped four major transfer faults within the KGF (Fig. 3). The Pelitliada Fault is a steep NNE-trending fault located near Kızıldere village. This fault is approximately 2 km long and exhibits a steep dip of 80°, with a dextral component, dipping eastward (Fig. 6e, f). The fault is exposed near Kızıldere village and strikes NNE, continuing northward with a trend that transitions from NNE to N–S, following a deeply incised valley. Similar to other transfer faults, it delimits the E–W trending normal faults. Fault-slip measurements on this fault are limited due to extensive deformation in the fault zone, which extends over more than 50 m. The average geometry of the fault is N15E/80SE, and the average rake of the slickensides is oriented 75°N (azimuth: 049N/72) (Fig. 6f).

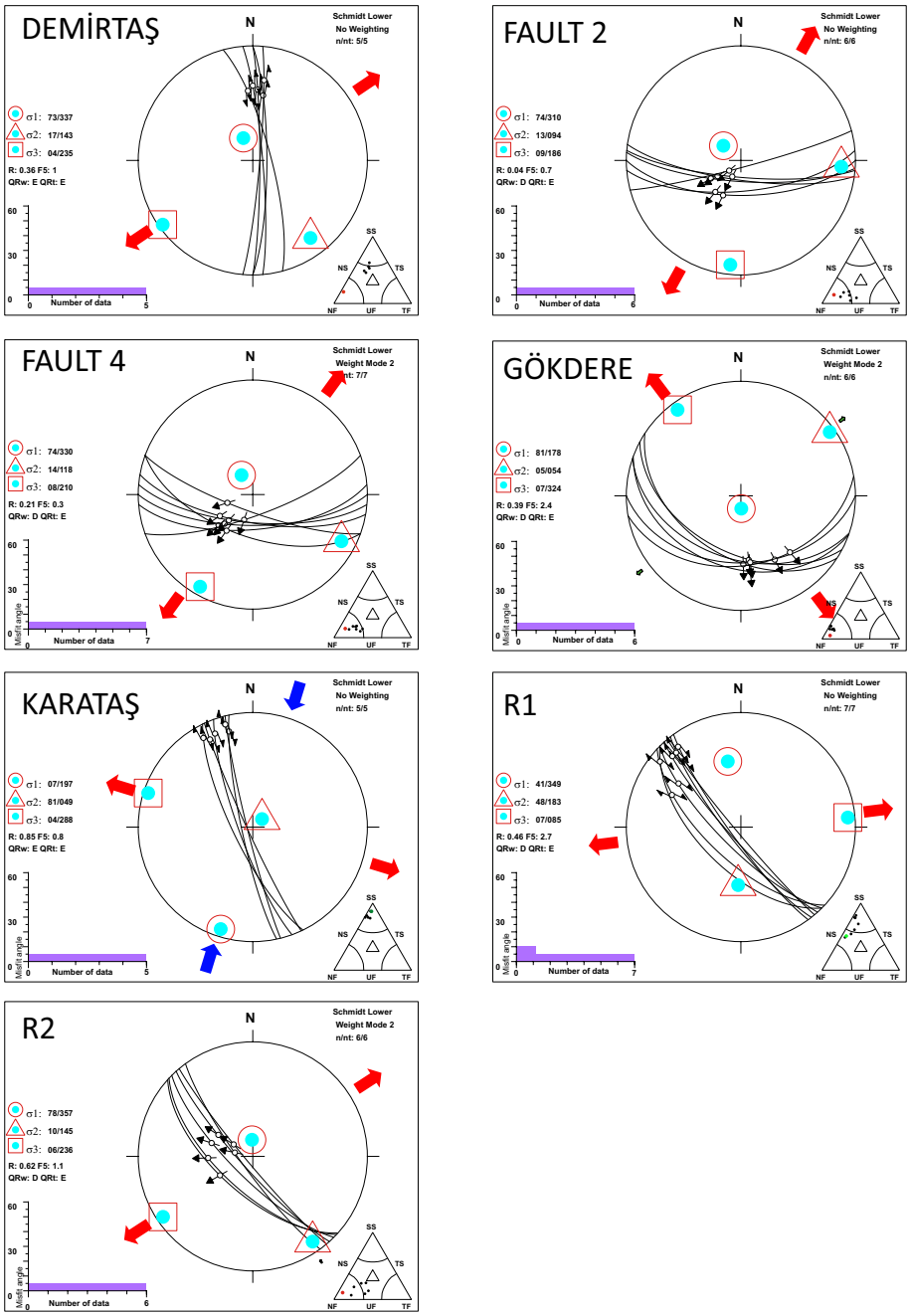


Fig. 7 Constructed paleostress configurations. *NF* normal fault, *SS* strike-slip fault, *TF* thrust fault, *n* number of data, σ1–σ2–σ3 maximum–intermediate–minimum principal stresses, *R* stress ratio (σ2–σ3)/(σ1–σ3)

This structure is a key component of the KGF, marking the western extent of the Kızılburun and Sazak formations (Fig. 3).

The Demirtaş Fault is a 2 km long, steep (77°E-85°E) normal fault with a slight sinistral component (Fig. 6c, d). It is prominently observed around Kızıldere village, where its eastward convex traces change from NNE to N–S trends as it extends northward. Similar to the Pelitliada Fault, it also delimits the E–W striking normal faults. Paleostress

Table 1 Details of the calculated paleostress orientations obtained from fault-slip data collected in the field

Site ID	Long	Lat	Fault name	n	σ_1		σ_2		σ_3		R	Regime
					P	D	P	D	P	D		
Demirtas	658767	4205375	Demirtaş	5	73	337	17	143	4	235	0.36	Extensional
Fault 4	658496	4204807	Buharkent	7	74	330	14	118	8	210	0.21	Extensional
Fault2	660912	4203480	Buharkent	6	74	310	13	94	9	186	0.04	Extensional
Gokdere	662832	4204809	Gökdere	6	81	178	5	54	7	324	0.39	Extensional
Karatas	664050	4205978	Karataç	5	7	197	81	49	4	288	0.85	Strike-slip
R1	662908	4204491	Gebeler	7	41	349	48	183	7	85	0.46	Extensional
R2	662908	4204491	Gebeler	6	78	357	10	145	6	236	0.62	Extensional

n number of data, *D* direction, *P* plunge, *R* stress ration [$R = (\sigma_2 - \sigma_3)/(\sigma_1 - \sigma_3)$]

configurations derived from the slickensides on this fault indicate NE–SW extension, with both normal and sinistral components of motion (Fig. 7 and Table 1).

The Gebeler Fault lies in the heart of the KGF and forms a 4 km wide deformation zone characterized by steep fault scarps, numerous hot springs and fumaroles, hydrothermally altered rocks, deeply incised valleys, and overprinting slickenlines indicating multiple phases of deformation (Fig. 8a–d). The main structure in this complex, outcropping near the energy plant, is a 3.3 km long, high-angle (80-86°), west-dipping normal fault with a strike-slip component, referred to as the Gebeler Fault (Fig. 3a). It exhibits two antithetic splay faults, labelled A and B on the geological map (Fig. 3a, b). These splay faults cut and displace both the metamorphic rocks and Miocene basin-fill deposits, both vertically and horizontally. Fault A is an NNE to NNW trending, 1.8 km long, steep (~75°) strike-slip fault dipping east. It displaces the Sazak and Kolankaya formations (Fig. 8a, b). Fault B, which is developed parallel to Fault A, is a 2 km long, steep (~75°) oblique fault dipping east, displacing the Kızılburun, Sazak, and Kolankaya formations. Along the main branch of the Gebeler Fault, two sets of overprinting slickenlines have been observed (Fig. 8c, d). The older set of slickenlines (R1) indicates dextral motion, while the younger set (R2) shows normal motion. Paleostress reconstructions suggest that these faults developed under ENE–WSW to E–W directed extension (Fig. 7 and Table 1).

The Karataş Fault is a 4.5 km long, steep west-dipping (76°-80°) dextral strike-slip fault (Fig. 6a, b). It juxtaposes the Sazak and Kolankaya formations both vertically and horizontally. It has three splay faults, labelled as C, D, and E on the geological map (Fig. 3). Fault C is a west-dipping fault, almost parallel to the Gebeler Fault. It is a 1.6 km long, steep (~70°) normal fault displacing the Sazak and Kolankaya formations. Fault D, located between the Gebeler and Karataş faults, is a steep (~75°) west-dipping normal fault with an NNE to NNW trend. Fault E is an east-dipping antithetic splay of the Karataş Fault, which displaces both Sazak and Kolankaya formations. It is 2 km long and exposed along a deeply incised valley. Paleostress configurations constructed from fault-slip data indicate that the Karataş Fault is a normal fault with a dextral strike-slip component, developed under NW–SW extension (Fig. 7 and Table 1).

Although the splay structures along these faults suggest a high normal slip component, the main displacement along the NE-trending transfer faults is characterized by a

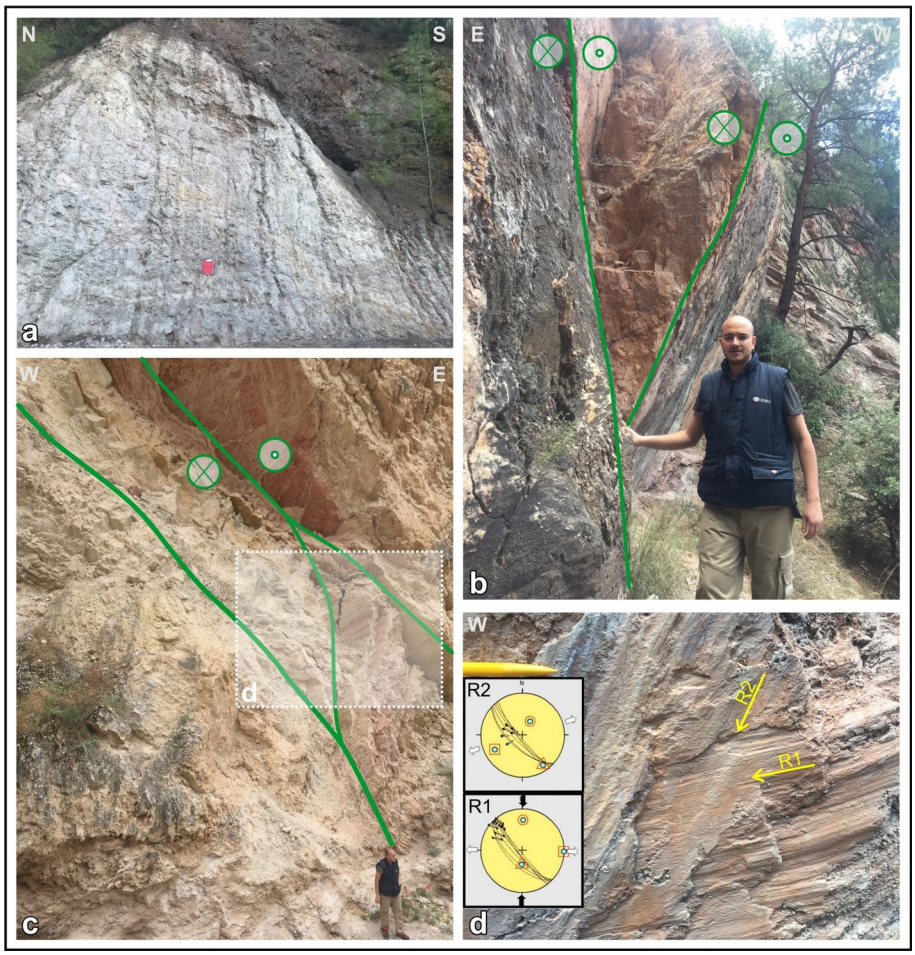


Fig. 8 **a-c** General views of the Gebeler Fault, and **d** a close-up view of the fault surface including two overprinting sets of slickenlines in Gebeler Valley (see text for details). R1 represents the older slickenline set showing dextral strike-slip faulting, while R2 shows the younger set showing oblique-slip faulting. Kinematic analysis for each faulting is given

dominant strike-slip component under regional extension (Figs. 2b and 3). These faults accommodate differential displacement between the E–W normal faults. In the study area, the NE-trending transfer faults occasionally cut and displace younger E–W trending normal faults, although they also delimit E–W faults in some locations. Based on field observations and seismic profiles, the 3D geometries of these faults on either side of the Büyük Menderes Graben have been interpreted (Fig. 3a). Key criteria for identifying these structures in the field include deeply incised valleys, presence of striated surfaces, steep fault scarps, sudden changes in slope, and juxtaposition of different stratigraphic units. The traces of most of these faults follow a curvilinear path to the north, which may suggest a listric geometry, though this is not observed in the seismic sections. The dominant role of these faults in the geothermal system is also evident from numerous surface manifestations, including hydrothermal alteration zones, lineated hot springs, and fumaroles.



Fig. 9 Field views of the E–W trending high-angle normal faults. **a** General view and kinematic analysis of the Gökdere Fault (GF), and **b-c** close-up views of slickenlines on the fault surface near Gökdere Village. **d** General view of the Buharkent Segment, **e** a close-up view and kinematic analysis of slickenlines of the F1 fault

E–W trending high-angle normal faults

The E–W (to WNW–ESE) faults represent segments of the Buharkent, Sarayköy, and Gökdere Faults, which play a key role in the development of the Büyük Menderes Graben (Emre et al. 2018; Sümer et al., 2020). The Gökdere Fault (GF in Fig. 3) is located along the northern margin of the Büyük Menderes Graben. It strikes almost E–W and extends for 7.5 km within the study area (Fig. 3a). This fault consists of a set of oblique-slip faults

that dip southwards at varying angles (Fig. 9a, b), with dip angles ranging from 40° to 60°S. It is traceable to the west, where it is limited by the Demirtaş Fault. The Gökdere Fault is offset by the NE-trending Gebeler Fault. To the northeast, it juxtaposes the Kızılburun and Sazak formations, while in the west, it juxtaposes the metamorphic basement and Miocene basin infill. Paleostress reconstruction based on fault-slip data from the Gökdere Fault suggests that it is an oblique-slip fault developed under N–S directed extension (Fig. 7 and Table 1). Field observations and geometric relationships in the geological map indicate that the Gökdere Fault is the oldest high-angle normal fault to displace both the basement rocks and the basin infill along the northern edge of the graben.

The youngest structures observed in the easternmost part of the graben are the branches of two fault segments: (i) the Buharkent Segment along the northern rim of the graben, and (ii) the Sarayköy Segment along the southern margin. The branches of the Buharkent Fault are mapped in detail and labelled F1 to F4 on the northern margin (Fig. 3a). In the study area, these branches form a 1–3 km wide, 12-km-long fault zone, predominantly consisting of E–W to NNW–ESE trending parallel normal faults (Fig. 9c–e). These faults, together with the NE–SW trending transfer faults, represent the youngest structures in the graben and control the deposition of Quaternary basin infill. The dip angle of these faults ranges from 60° to 85°, with most dipping around ~ 65° (Fig. 9d). The faults displace the basement rocks, graben deposits, and typically NE-trending transfer faults, with minor lateral components observed in certain places. Paleostress reconstruction from kinematic data on the Buharkent Segment indicates NE–SW directed extension (Fig. 7 and Table 1).

The Sarayköy Segment has two main fault branches in the study area (Fig. 3a). These branches, mapped as S1 and S2, create a deformation zone approximately 5 km long and 2 km wide along the southern edge of the graben. These faults dip towards the north, producing a step-like topography, which mirrors the geometry observed on the northern conjugate margin.

Our field observations suggest that the E–W trending high-angle faults are primarily normal faults with right-lateral oblique components, developed under the recent extensional regime of Western Anatolia (Fig. 7 and Table 1). On both margins of the graben, these faults form a set of parallel active faults, exhibiting a planar geometry at depth as interpreted from seismic profiles. The ages of these faults display a step-like morphology, becoming progressively younger from the margin towards the basin centre. These faults interact with the NE-trending faults and cross-faults, which exhibit strong lateral components, indicating that these cross-faults act as transfer faults. These transfer faults delimit the E–W faults laterally and accommodate differential extensional deformation along the graben-bounding faults. As shown in Fig. 9a, steep fault scarps, contorted stream courses, and widespread alluvial apron deposition facilitate the recognition of these features in the field (Fig. 9a, b).

3D Modelling

Defining the stratigraphic and tectonic boundaries, the distribution of cap and reservoir rocks, and the structural network of faults are essential elements for effective geothermal exploration. To this end, 3D structural and geological modelling has been employed to gain a comprehensive understanding of the Kızıldere Geothermal Field (KGF). The

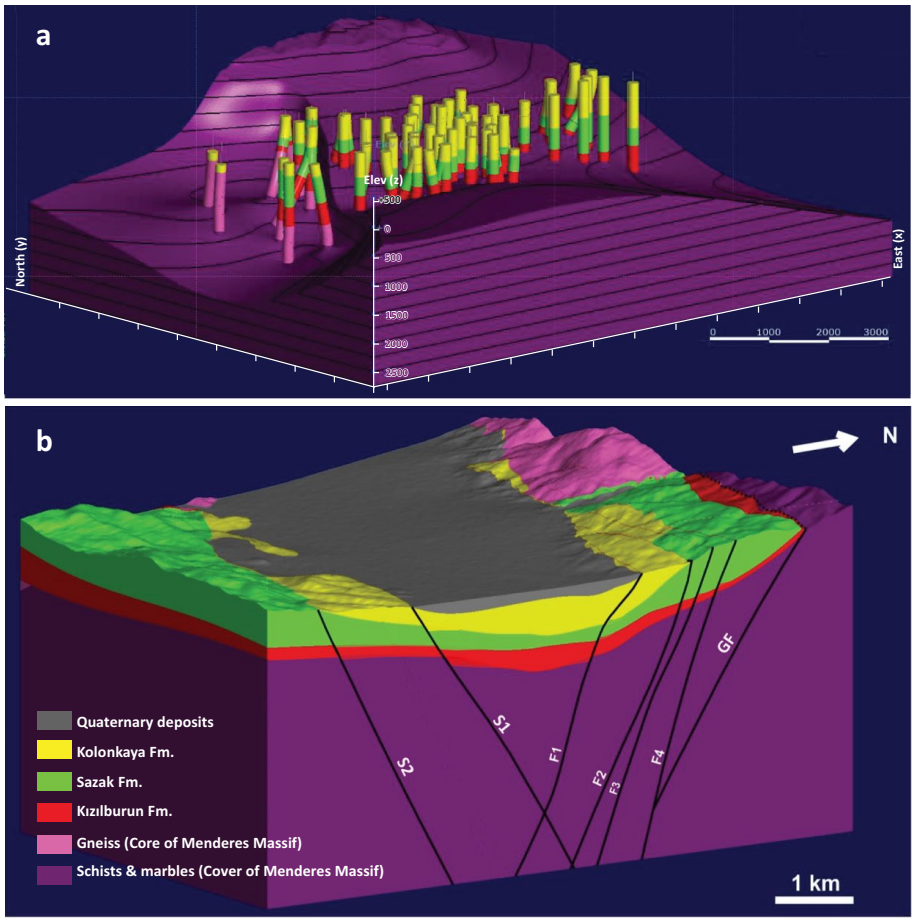


Fig. 10 3D solid models of the study area: **a** well data and preliminary lithological model and **b** structural model of the Kızıldere Geothermal Field. See Fig. 3 for the location of the models

foundation of these models is based on our detailed field observations and borehole data (Fig. 10a), with seismic sections serving as complementary sources of information, though their inclusion is restricted due to confidentiality concerns. A total of 76 boreholes were integrated into the model to interpret the stratigraphic and tectonic horizons and to map the subsurface fault geometries.

During drilling, the loss of mud circulation was encountered, which indicated the presence of voids in the rock. These voids could represent fissures, fractures, underground caverns, and, importantly, faults. When combined with field observations, such drilling data provide a powerful tool for interpreting the subsurface continuation of faults. The 3D structural and geological models of the KGF were generated using Leapfrog Geothermal©, a 3D modelling and visualization software.

The 3D lithological solid model was constructed in two main steps: (i) the initial volumes were generated using borehole data, and (ii) the model was refined and edited based on field observations to ensure a more realistic representation of the subsurface (Fig. 10). The boundary of the model is constrained to the seismic and well coverage area while field measurements are used to understand the characteristics and kinematics of the faults encountered on the seismic lines and the faults. The

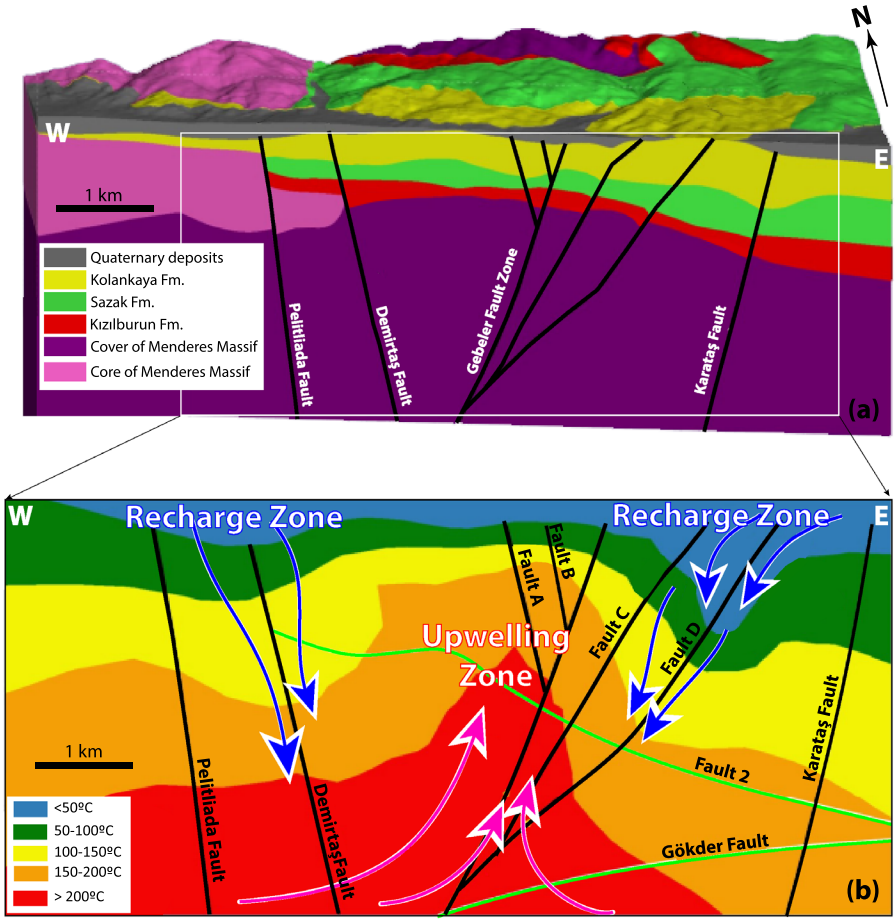


Fig. 11 3D lithological model and temperature distribution in the same section. **a** 3D model and a cross-section showing major N–S trending faults. Note ~ 800 m vertical offset along the Pelitliada Fault. **b** Temperature distribution in the same section above. Note that the Gebeler Fault is the most favourable structure controlling the recharging and upwelling of geothermal fluids. See Fig. 3 for the location of the model

intervals where mud loss occurred during drilling are used to infer the position of the high-permeability reservoir levels. The modelled E–W trending fault planes include F1 to F4 (Fig. 3), with the Gökdere Fault located along the northern margin of the Büyük Menderes Graben (Figs. 3 and 10b). Additionally, two fault planes, S1 and S2, located on the southern margin, were also included in the model. However, we were unable to determine the exact cross-cutting relationships between the southern and northern E–W trending faults in the field; however, their relationship in the 3D model is based on seismic sections.

The structure that limits the western extent of these formations is the NE-trending Pelitliada Fault. The area to the east of the Pelitada fault is a downthrown block, and all the basin-fill units are encountered in the wells. However, only the Kolonkaya Formation is encountered in the west, the foot-wall block of the Pelitada fault. The

thickness of the basin infill units increases towards the Pelitada fault, implying syn-depositional activity of the fault. The Tosunlar Formation and Quaternary deposits were not separately modelled; instead, a combined volume referred to as the "Quaternary Basin Fill" was created to represent these units (Fig. 11a).

In addition to the lithological and structural modelling, static temperatures obtained from reservoir tests were used to develop a 3D temperature model (Fig. 11b). Visualizing the temperature distribution within the KGF is crucial for identifying favourable geothermal structures and for understanding fluid circulation patterns. The thermal model revealed higher temperatures in both the western and central parts of the field, with the highest temperature zone situated within the Gebeler Fault.

Discussion

Geothermal fields are generally associated with regions where an elevated geothermal gradient is present due to magmatic activity or regional extensional and transtensional tectonic structures (e.g., Brogi et al., 2003; Meixner et al. 2016; Perez-Flores et al. 2017; 2018; Glaas et al. 2021; Dezayes et al. 2021; Liotta et al. 2021; Marchesini et al. 2025). In these regions, successful geothermal exploration requires a comprehensive understanding of several factors, including the heat source, the distribution of cap and reservoir rocks, the locations of upwelling and recharge zones, and the structural controls on geothermal fluid flow. The Kızıldere Geothermal Field (KGF) stands as one of the highest-enthalpy geothermal fields, with an electricity production capacity exceeding 360 MW. It is developed in an extensional setting with no direct association to nearby magmatic systems. We propose that the heat is primarily provided by an elevated geothermal gradient resulting from crustal thinning, regional stretching, and young core-complex evolution (see Roche et al. 2019 and references therein).

Reservoir characteristics

The Kızıldere Geothermal Field (KGF) exhibits all essential components of a geothermal system. Effective resource exploitation requires a comprehensive understanding of the three-dimensional distribution of reservoir and cap rocks, up flow and discharge zones, and the structural framework controlling fluid flow.

The most productive reservoir rocks in the KGF are a massive marble unit, typically encountered at depths exceeding 3000 m, where the highest-temperature and maximum-discharge wells are located. Quartzite layers may locally act as secondary reservoirs; however, marbles remain the primary productive horizons due to their brittle behaviour and karstic development. It is well established that the circulation of hot, acidic geothermal fluids through faulted and highly fractured carbonates promotes leaching and karstification, which substantially enhance reservoir permeability and storage capacity.

The secondary reservoir consists of the upper few hundred metres of metamorphic rocks that have been structurally modified by a detachment fault. A considerable portion of current production wells operate from this level as well.

The tertiary reservoir rocks involve Sazak Formation, dominantly composed of limestone. The presence of fumaroles on this unit confirms its geothermal activity. Despite

its intermediate temperatures, this reservoir is still utilized for production, with injection wells predominantly targeting this formation.

During the drilling several metres of underground cave systems associated with faults, with "bit drops" are reported. This observation suggests the existence of significant karstic developments, likely in the form of fractures or caverns.

Lithologies characterized by low porosity and permeability can function as a cap rock. In KGF, the gneisses and various foliated, non-carbonate lithologies of the Menderes Massif provide excellent caprock for the underlying marble reservoirs, with its thick, hundreds-of-metres-thick schist units serving as a regional seal. Similarly, the claystone intervals of the Kızılburun Formation possess cap rock properties, although their lateral extent is limited (Fig. 11). On the other hand, the Kolankaya Formation is a widespread, impermeable unit with thick, consistent layers of clay-rich marl. It acts as the regional cap rock for the KGF, enveloping both the Sazak Formation and the reservoirs within the basement (Menderes Massif), thereby preventing the upward migration of geothermal fluids and insulating heat within the system.

Contrary to previous studies in the area, our findings, based on detailed field observations and borehole data, suggest the presence of an intra-basinal unconformity between the Kolankaya Formation and the older graben infill (Fig. 11a). The Pelitlada Fault limits the western extension of the older Miocene deposits, a feature that was confirmed by seismic data, which shows the Pelitlada Fault is a cross-fault that formed under a WNW–ESE-directed extension. Although the present activity of the Pelitada Fault remains uncertain, it still plays an important role in the percolation of geothermal fluids, as evidenced by the temperature distribution within the basin (Fig. 11b). Several wells were drilled in the Eski Savcılı area, located outside to the west of the study area (Fig. 3a), in an attempt to assess the geothermal potential of this region. However, the wells failed to encounter significant geothermal fluids, despite the location of these wells along the major basin-bounding fault. The vertical throw along the Pelitlada Fault is approximately 400 m, as indicated by the vertical offset of the basement rocks on both sides of the fault. Elsewhere, the offset reaches up to approximately 800 m.

It appears that the western boundary of the KGF is defined by the Pelitlada Fault, while the eastern boundary is constrained by the Karataş Fault.

Structural control

Active extensional faults are often the most promising sites for geothermal exploration in extensional terranes. A general guideline is to prioritize active faults because they enhance porosity and permeability through repeated fracturing and movement. In contrast, inactive faults are typically less effective since the fractures within their zones are often sealed or closed. Additionally, fault zones frequently develop gouge at shallow depths, which can further impede fluid flow.

In well-studied geothermal systems, the most favourable zones for fluid percolation are rarely associated with simple dip-slip normal faults, which often act as barriers to vertical flow (Cox 1999; 2016). Instead, high-angle transfer faults, particularly in extensional settings, form near-vertical, interconnected fracture networks (Fig. 12) that promote vertical fluid migration. Such structural configurations have been documented in geothermal fields in Italy (Brogi et al., 2003, 2005), Iceland (Liotta et al.

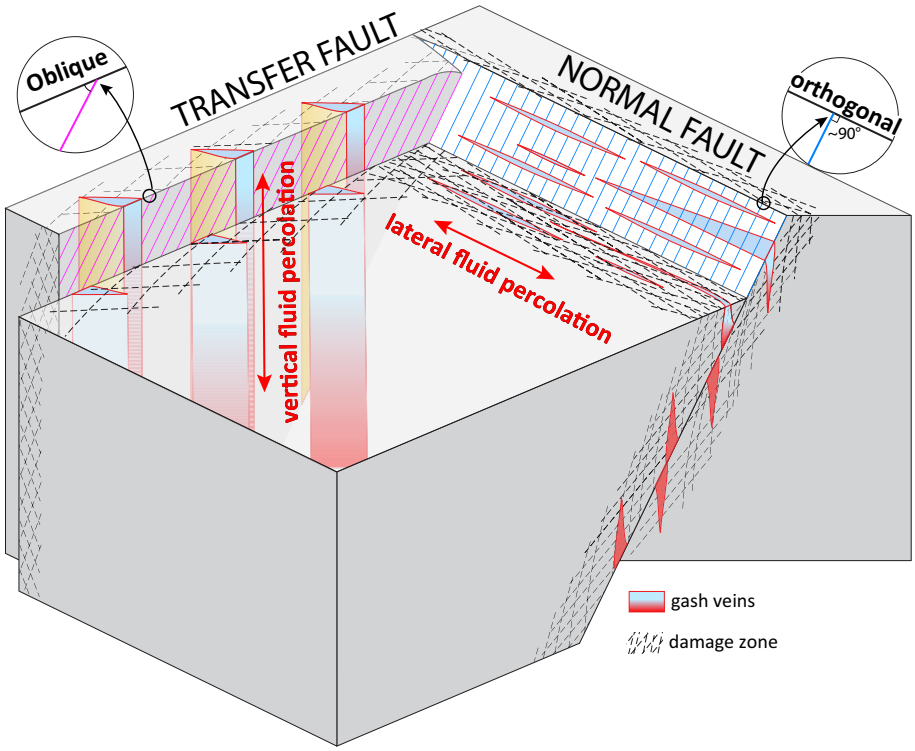


Fig. 12 Conceptual model illustrates the geometry and role of extension veins along normal and transfer faults. Note that transfer faults, which display dominant strike-slip components, generate near-vertical open-mode fractures that facilitate vertical fluid percolation, while normal faults exhibit nearly orthogonal slip vectors (slickensides), and the long axes of the extension veins are oriented almost parallel to the fault strike, promoting lateral fluid migration rather than vertical migration

2021), and the Denizli Basin in western Türkiye (Brogi et al. 2014, 2021; Alçiçek et al. 2018), located approximately 20 km east of the KGF. Notably, the well-characterized geothermal fields along the northern margin of the Denizli Basin (e.g., Kamara and Gölemezli) are similarly controlled by normal and transfer faults (Brogi et al. 2021).

Paleostress analysis of kinematic data collected in the study area reveals that a multidirectional extensional regime, accompanied by localized compression, prevailed during the pre-Quaternary period (Fig. 7). During this time, low-angle normal faults and NE-trending strike-slip faults were active in the westernmost part of the Büyük Menderes Graben (Sümer et al., 2020). Variations in paleostress directions along the NE-trending faults can be attributed to local rotations induced by younger faulting and cross-cutting relationships (Fig. 3). In the Quaternary, the geothermal area was first influenced by NW–SE-trending extension, which produced the Gökdere Fault, followed by a transition to NE–SW-trending extension that led to the formation of the Buharkent Segment (Figs. 7 and 13). These paleostress trends are consistent with previously published paleostress and strain data (Sümer et al., 2020; Özkaptan et al. 2021).

The Kızıldere Geothermal Field (KGF) is located along the northern flank of an actively developing graben and is dominated by E–W-striking normal and cross-faults (Figs. 2 and 3). These structures likely provide the primary permeability pathways for

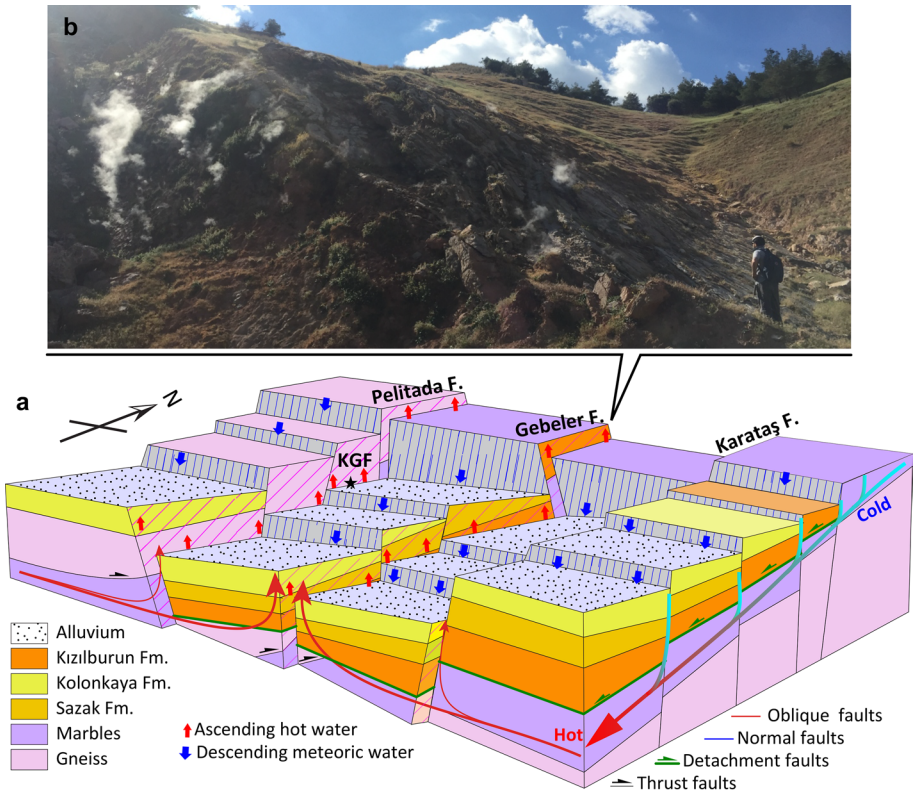


Fig. 13 **a** Conceptual 3D geothermal model illustrating the fluid percolation and temperature distribution in the Kızıldere Geothermal Field. Note that both E–W- and NE-trending faults are used for recharging while NE-trending transfer faults are used for upwelling of hot geothermal fluids. **b** Field photo of a fumarole that occurred along the Gebeler Fault, a NE-trending transfer fault (looking west)

the geothermal system, particularly along the Gebeler Fault. This fault is a dilatational, strike-slip–dominated transfer fault that forms a complex deformation zone, composed of multiple antithetic and synthetic splays merging into a single shear zone at depth. Along strike-slip faults, dilatational fractures typically develop with near-vertical long axes, enhancing upward fluid migration. Figure 12 illustrates simplified gash-vein geometries: transfer faults generate near-vertical openings that favour vertical fluid percolation, whereas normal faults predominantly promote lateral fluid migration, as their associated gash fractures are oriented parallel to the fault strike. Such fracture configurations likely facilitated the ascent of geothermal fluids along the Gebeler Fault (Fig. 11b).

Despite its relatively small visible offset compared to other NE-trending transfer faults, the Gebeler Fault stands out as one of the hottest structural zones in the area. At its eastern termination, it interacts with Fault 2, the northern bounding fault of the Büyük Menderes Graben (Fig. 11b). To the north of this intersection, the structural pattern is dominated by closely spaced E–W faults with subordinate NE-trending faults. We suggest that the interaction of these fault sets created sufficient permeability for geothermal fluid ascent. In contrast, the Pelitlada–Demirtaş and Karataş faults, which exhibit the largest vertical displacements in the area, likely serve as primary recharge

(fluid-descending) structures. Conversely, smaller-offset faults, such as the Gebeler Fault and associated E–W faults, appear to control fluid up flow (Figs. 11b and 13).

Geochemical studies conducted by Karakuş and Şimşek (2013) indicate that the KGF fluids are predominantly of meteoric origin. The primary source of descending water appears to be the Büyük Menderes River, which sustains high groundwater levels that promote the upflow of heated fluids along marginal faults that are not directly intersected by the river (Fig. 3). Consequently, ascending fluids are less likely to mix with descending groundwater along the main graben-bounding faults (Fig. 13). Moreover, the Pelitlada–Demirtaş and Karataş faults extend into the horst blocks flanking the graben, which likely receive substantial recharge from winter and spring precipitation and snowmelt. In contrast, the Gebeler Fault appears to lack significant direct recharge but nevertheless serves as a critical conduit for the ascent of hot geothermal fluids (Fig. 13).

Implications for geothermal productivity

The role of transfer fault zones in the development of geothermal fields is well established (e.g., Cameli et al. 1993; Liotta et al. 2021, and references therein). In post-collisional extensional settings such as western Anatolia, crustal thinning and the associated high heat flow constitute the primary sources of geothermal energy, even when deep-seated magmatic intrusions are not present. Within such settings, damage zones of normal faults create permeability that allows meteoric water to percolate downward, while ascending thermal fluids migrate laterally into shallow reservoirs, as observed at the KGF (Fig. 13).

Deeply connected fissures and open-mode fractures within near-vertical transfer fault zones provide highly permeable conduits that facilitate the rapid ascent of hot fluids to the surface (Fig. 12). In other words, normal faults predominantly control recharge by meteoric waters and lateral fluid migration (Figs. 12 and 13). The intersections of normal and transfer fault zones create "permeability sweet spots," particularly when suitable reservoirs are present—such as fractured clastic units or easily dissolvable carbonate and evaporite sequences.

At the KGF, all these conditions converge to generate a highly productive geothermal system. Graben-bounding normal faults provide the primary pathways for meteoric recharge. Reservoirs are hosted within marbles, fractured quartzites, and carbonate-rich basin-fill units, whereas gneisses, fine-grained clastic, and mudstones act as effective cap rocks. Transfer faults such as the Gebeler Fault supply vertical conduits for thermal fluid ascent. Consequently, the most productive zones—or "sweet spots"—occur where normal and transfer faults intersect in the presence of suitable reservoir and caprock configurations. This structural and lithological interplay ultimately governs the high productivity of the KGF.7.

Conclusions

This study provides an integrated structural and hydrogeological assessment of the Kızıldere Geothermal Field (KGF), highlighting the geological factors that govern its high productivity. Key conclusions are as follows:

- Faults are the fundamental elements of the KGF geothermal system. They govern the percolation of meteoric waters, control the distribution of reservoir rocks, and enhance secondary porosity and permeability.
- Field observations, borehole data, and 3D reservoir modelling demonstrate that the Gebeler Fault is the most productive structure in the field. This fault forms a dilatational transfer zone where E–W-trending normal graben faults intersect with near-vertical NE-trending transfer faults, creating a highly fractured volume that facilitates both downward recharge and upward thermal fluid migration.
- The highest geothermal productivity occurs at the intersections of graben-bounding normal faults and transfer faults. Normal faults provide pathways for meteoric recharge and lateral fluid migration, while transfer faults create vertical conduits for rapid thermal fluid ascent. This structural interaction generates permeability "sweet spots" when underlain by suitable reservoirs—fractured marbles, quartzites, and carbonate-rich basin fill—and sealed by low-permeability units such as schists, gneisses, and mudstones.
- The KGF exemplifies how crustal thinning, elevated regional heat flow, and integrated fault networks produce highly productive geothermal systems without shallow magmatic heat sources. Identifying the 3D geometry of normal and transfer faults, along with the distribution of reservoir and cap rocks, is critical for successful exploration and development in similar extensional terranes.

Overall, the structural-hydrogeological interplay at KGF illustrates that the most productive geothermal zones emerge where lithology and fault architecture combine to maximize permeability. These insights provide a framework for targeting "sweet spots" in other high-enthalpy geothermal systems in Western Anatolia and comparable extensional regions worldwide.

Acknowledgements
This study is part of the first author's M.Sc. thesis and was supported by Zorlu Energy Company. We would like to express our appreciation for the assistance provided by the staff at Zorlu Energy, including Muzaffer Sağanak Cavunt, Metin Yazman, Ali Kindap, Erinç Tonguç, Abdülkadir Yılmaz, Öncü Demircioğlu, Bahadır Erdoğan, Selcen Gündüz Görgülü, Emre Cem Emiroğlu, Uğur Kaygısız, Gürhan Osmanoğlu, and Koray Öztürk. We also extend our gratitude to the hospitable people of Buharkent village. This research was partly supported by the Scientific and Technical Research Council of Turkey (TÜBITAK Research Grant 120Y133).

Author contributions
NK, BU: conceived and designed the study. BA and BU: collected the data, BA & BU: processed the data. BA: wrote the initial manuscript draft & performed the analysis. All authors contributed to interpretation of the results, revised the manuscript, and approved the final version.

Data availability
No datasets were generated or analysed during the current study.

Declarations

Ethics approval and consent to participate
The authors declare no conflicts of interest. This study did not involve human, animal, or organic subjects. The authors affirm adherence to ethical standards and take full responsibility for the integrity of the research and manuscript.

Competing interests
The authors declare no competing interests.

Received: 14 May 2025 Accepted: 8 September 2025
Published online: 24 September 2025

References

Akkus I, Akilli H, Ceyhan S, Dilemre A, Tekin Z. Türkiye Jeotermal Kaynaklari Envanteri (Inventory of Geothermal Resources of Türkiye). General Directorate of Mineral Research and Exploration (MTA), Ankara, Türkiye.

Alçiçek H, Varol B, Özkul M. Sedimentary facies, depositional environments and palaeogeographic evolution of the Neogene Denizli Basin, SW Anatolia, Türkiye. Sediment Geol. 2007;202(4):596–637. https://doi.org/10.1016/j.sedgeo.2007.06.002.

Alçiçek MC, Brogi A, Capezzuoli E, Liotta D, Meccheri M. Superimposed basin formation during Neogene-Quaternary extensional tectonics in SW-Anatolia (Türkiye): insights from the kinematics of the Dinar Fault Zone. Tectonophysics. 2013;608:713–27. https://doi.org/10.1016/j.tecto.2013.08.008.

Alçiçek H, Wesselingh FP, Alçiçek MC. Paleoenvironmental evolution of the late Pliocene–early Pleistocene fluvio-deltaic sequence of the Denizli Basin (SW Türkiye). Palaeogeogr Palaeoclimatol Palaeoecol. 2015;437:98–116.

Alçiçek H, Bülbül A, Alçiçek MC. Hydrogeochemistry of the thermal waters from the Yenice geothermal field (Denizli Basin, Southwestern Anatolia, Türkiye). J Volcanol Geotherm Res. 2016;309:118–38.

Alçiçek H, Bülbül A, Capezzuoli E, Brogi A, Liotta D, Meccheri M, et al. Origin, evolution and geothermometry of thermal waters in the Gölemezli Geothermal Field, Denizli Basin (SW Türkiye). J Volcanol Geotherm Res. 2018;349:1–30.

Alçiçek H, Bülbül A, Yavuzer İ, Alçiçek MC. Hydrogeochemical and isotopic assessment and geothermometry applications of the Karahayıt Geothermal Field (Denizli Basin, SW Anatolia, Türkiye). Hydrogeol J. 2019a;27:1791–816.

Alçiçek H, Bülbül A, Yavuzer İ, Alçiçek MC. Origin and evolution of the thermal waters from the Pamukkale Geothermal Field (Denizli Basin, SW Anatolia, Türkiye): insights from hydrogeochemistry and geothermometry. J Volcanol Geotherm Res. 2019b;372:48–70.

Balkan-Pazvantoğlu E, Erkan K, Şalk M, Akkoyunlu BO, Tayanç M. Surface heat flow in western Anatolia (Türkiye) and implications to the thermal structure of the Gediz Graben. Turk J Earth Sci. 2021;30:991–1007. https://doi.org/10.3906/yer-2105-28.

Batini F, Brogi A, Lazzarotto A, Liotta D, Pandeli E. Geological features of Larderello-Travale and Mt. Amiata geothermal areas (southern Tuscany, Italy). Episodes. 2003;26(3):239–44.

Biryol CB, Beck SL, Zandt G, Özacar AA. Segmented African lithosphere beneath the Anatolian region inferred from teleseismic P-wave tomography. Geophys J Int. 2011;184:1037–57.

Bozcu M. Geology of neogene basins of Buldan-Saricaova region and their importance in western Anatolia Neotectonics. Int J Earth Sci. 2010;99(4):851–61. https://doi.org/10.1007/s00531-009-0431-7.

Bozkurt E. Timing of extension on the Büyük Menderes graben, western Türkiye, and its tectonic implications. Geol Soc. 2000;173(1):385–403. https://doi.org/10.1144/gsl.sp.2000.173.01.18.

Bozkurt E. Neotectonics of Türkiye - a synthesis. Geodinam Acta. 2001;14:3–30.

Bozkurt E, Oberhänsli R. Menderes massif (Western Türkiye): structural, metamorphic and magmatic evolution - a synthesis. Int J Earth Sci. 2001;89(4):679–708. https://doi.org/10.1007/s005310000173.

Bozkurt E, Park LR. Southern Menderes Massif: an incipient metamorphic core complex in western Anatolia, Türkiye. J Geol Soc. 1994;151(2):213–6.

Brogi A, Lazzarotto A, Liotta D, Ranalli G. Extensional shear zones as imaged by reflection seismic lines: theLarderello geothermal field (central Italy). Tectonophysics 2003;363(1-2):127-139

Brogi A, Capezzuoli E, Alçiçek MC, Gandin A. Evolution of a fault-controlled travertine fissure-ridge in the western Anatolia extensional province: the Çukurbağ fissure-ridge (Pamukkale, Türkiye). J Geol Soc. 2014;171:425–41.

Brogi A, Alçiçek MC, Yalçıner CC, Capezzuoli E, Liotta D, Meccheri M, et al. Hydrothermal fluids circulation and travertine deposition in an active tectonic setting: insights from the Kamara geothermal area (western Anatolia, Türkiye). Tectonophysics. 2016;680:211–32.

Brogi A, Alçiçek MC, Liotta D, Capezzuoli E, Zucchi M, Matera PF. Step-over fault zones controlling geothermal fluid-flow and travertine formation (Denizli Basin, Türkiye). Geothermics. 2021;89:101941.

Brogi A, Israde I, Árnadóttir S, Capezzuoli E. Tectonic control on travertine and silica sinter deposition in oceanic transform-fault setting: the case of the Lýsuskarð volcano-geothermal area, Snæfellsnes Peninsula, Iceland. Int Geol Rev. 2023;65(21):3287–310. https://doi.org/10.1080/00206814.2023.2180779.

Brogi, A., Capezzuoli, E., Costantini, A., Gandin, A. and Lazzarotto, A., 2005. Tectonics and travertines relationships in the Rapolano Terme area (Northern Apennines, Italy). In Proceedings 1st International Symposium on Travertine (pp. 142–148). Kozan Ofset Matbaacilik San. ve Tic. Ltd. Şti.

Burke K, Sengör C. Tectonic escape in the evolution of the continental crust. Reflect Seismol: the Continental Crust. 1986;14:41–53.

Cameli GM, Dini I, Liotta D. Upper crustal structure of the Larderello geothermal field as a feature of post-collisional extensional tectonics (Southern Tuscany, Italy). Tectonophysics. 1993;224:413–23. https://doi.org/10.1016/0040-1951(93)90041-H.

Candan O, Dora O, Oberhänsli R, Çetinkaplan M, Partzsch J, Warkus F, et al. Pan-African high-pressure metamorphism in the Precambrian basement of the Menderes Massif, western Anatolia, Türkiye. Int J Earth Sci. 2001;89(4):793–811. https://doi.org/10.1007/s005310000097.

Candan O, Koralay OE, Akal C, Kaya O, Oberhänsli R, Dora OÖ, et al. Supra-Pan-African unconformity between core and cover series of the Menderes Massif/Türkiye and its geological implications. Precambrian Res. 2011;184(1–4):1–23. https://doi.org/10.1016/j.precamres.2010.09.010.

Capezzuoli E, Ruggieri G, Rimondi V, Brogi A, Liotta D, Alçiçek MC, et al. Calcite veining and feeding conduits in a hydrothermal system: insights from a natural section across the Pleistocene Gölemezli travertine depositional system (western Anatolia, Türkiye). Sediment Geol. 2018;364:180–203.

Çetinkaplan M, Candan O, Oberhänsli R, Sudo M, Cenki-Tok B. P-T–t evolution of the Cycladic Blueschist Unit in Western Anatolia/Türkiye: geodynamic implications for the Aegean region. J Metamorph Geol. 2020;38(4):379–419.

Cox SF. Deformational controls on the dynamics of fluid flow in mesothermal gold systems. Geol Soc. 1999;155(1):123–40.

Cox SF. Injection-driven swarm seismicity and permeability enhancement: implications for the dynamics of hydrothermal ore systems in high fluid-flux, over pressured faulting regimes—an invited paper. Econ Geol. 2016;111(3):559–87.

Delvaux D, Sperner B. Stress tensor inversion from fault kinematic indicators and focal mechanism data: the TENSOR program. In: Nieuwland D, editor. new insights into structural interpretation and modelling. Geological Society. London: Special Publications; 2003. p. 75–100.
Deng H, Kusky T, Bozkurt E, Chen C, Wang L, Dong Z, et al. Sr–Nd–Ca isotopic variations of Cenozoic calc-alkaline and alkaline volcanic rocks above a slab tear in Western Anatolia, Türkiye. GSA Bull. 2024;136(1–2):201–16.
Dewey JF, Şengör AMC. Aegean and surrounding regions complex multiplate and continuum tectonics in a convergent zone. Geol Soc Am Bull. 1979;90:8492. https://doi.org/10.1130/00167606.
Dezayes C, Lerouge C, Innocent C, Lach P. Structural control on fluid circulation in a graben system: constraints from the Saint Pierre Bois quarry (Vosges, France). J Struct Geol. 2021;146:104323.
Dickson, M.H. and Fanelli, M., 2018. What is geothermal energy? In Renewable Energy 1st Edition, 302- 328.
Dolmaz MN, Hisarli ZM, Ustaömer T, Orbay N. Curie point depths based on spectrum analysis of aeromagnetic data, West Anatolian extensional province, Türkiye. Pure Appl Geophys. 2005;162(3):571–90.
Emre Ö, Duman TY, Özalp S, Şaroğlu F, Olgun Ş, Elmacı H, et al. Active fault database of Türkiye. Bull Earthquake Eng. 2018;16(8):3229–75.
Erdoğan B, Güngör T. The problem of the core-cover boundary of the Menderes Massif and an emplacement mechanism for regionally extensive gneissic granites, Western Anatolia (Türkiye). Turk J Earth Sci. 2004;13:15–36.
Erkan K. Crustal heat flow measurements in western Anatolia from borehole equilibrium temperatures. Solid Earth Discuss. 2014;6(1):403–26. https://doi.org/10.5194/sed-6-403-2014.
Erkan K. Geothermal investigations in western Anatolia using equilibrium temperatures from shallow boreholes. Solid Earth. 2015;6(1):103–13. https://doi.org/10.5194/se-6-103-2015.
Eski S, Sözbilir H, Uzel B, Özkaymak Ç, Sümer Ö. Gölmarmara Fayı'nın Morfotektonik Evriminin CBS Tabanlı Yöntemlerle Araştırılması, Gediz Grabeni, Batı Anadolu. Türkiye Jeoloji Bülteni. 2020;63(3):345–72.
Faulds JE, Bouchot V, Moeck I, Oğuz K. Structural controls of geothermal systems in western Türkiye: a preliminary report. Geother Resour Council Trans. 2009;33(2009):375–82.
Gessner K, Piazolo S, Güngör T, Ring U, Kroner A, Passchier CW. Tectonic significance of deformation patterns in granitoid rocks of the Menderes nappes, Anatolide belt, southwest Türkiye. Int J Earth Sci. 2001;89:766–80.
Glaas C, Vidal J, Genter A. Structural characterization of naturally fractured geothermal reservoirs in the central Upper Rhine Graben. J Struct Geol. 2021;148:104370.
Gudmundsson A. Transport of geothermal fluids along dikes and fault zones. Energies. 2022. https://doi.org/10.3390/en15197106.
Gülyüz N, Gülyüz E, Karaoğlan F, Kuşcu İ. Low temperature thermochronology reveals tilting of crystalline bodies, Halilaga porphyry Cu–Au deposit, NW Anatolia: implications for exploration of porphyry copper deposits and interpretation of low-temperature thermochronology data for regional tectonics. Ore Geol Rev. 2024;166:105958.
Gürer ÖF, Sarıca-Filoreau N, Özburan M, Sangu E, Doğan B. Progressive development of the Büyük Menderes Graben based on new data, western Türkiye. Geol Mag. 2009;146(5):652–73. https://doi.org/10.1017/s0016756809006359.
Hetzel R, Ring U, Akal C, Troesch M. Miocene NNE-directed extensional unroofing in the Menderes Massif, southwestern Türkiye. J Geol Soc Lond. 1995;152:639–54.
Homberg C, Bergerat F, Angelier J, Garcia S. Fault interaction and stresses along broad oceanic transform zone: Tjörnes Fracture Zone, north Iceland. Tectonics. 2010. https://doi.org/10.1029/2008tc002415.
Işık V, Tekeli O. Late orogenic crustal extension in the northern Menderes massif (western Türkiye): evidence for metamorphic core complex formation. Int J Earth Sci. 2001;89:757–65.
Jolivet L, Menant A, Roche V, Le Pourhiet L, Maillard A, Augier R, et al. Transfer zones in Mediterranean back-arc regions and tear faults. BSGF-Earth Sci Bull. 2021;192(1):11.
Karabulut H, Paul A, Özbakır AD, Ergün T, Şentürk S. A new crustal model of the Anatolia-Aegean domain: evidence for the dominant role of isostasy in the support of the Anatolian plateau. Geophys J Int. 2019;218(1):57–73.
Karakuş H, Şimşek Ş. Tracing deep thermal water circulation systems in the E-W trending Büyük Menderes Graben, western Türkiye. J Volcanol Geotherm Res. 2013;252:38–52.
Kaya A. The effects of extensional structures on the heat transport mechanism: an example from the Ortakçı geothermal field (Büyük Menderes Graben, SW Türkiye). J Afr Earth Sci. 2015;108:74–88. https://doi.org/10.1016/j.jafrearsci.2015.05.002.
Kaymakci N. Kinematic development and paleostress analysis of the Denizli Basin (Western Türkiye): implications of spatial variation of relative paleostress magnitudes and orientations. J Asian Earth Sci. 2006;27(2):207–22. https://doi.org/10.1016/j.jseaes.2005.03.003.
Kaymakcı N, Langereis C, Özkaptan M, Özacar AA, Gülyüz E, Uzel B, et al. Paleomagnetic evidence for upper plate response to a STEP fault, SW Anatolia. Earth Planet Sci Lett. 2018;498:101–15.
Khodayar M, Björnsson S. Conventional geothermal systems and unconventional geothermal developments: an overview. Open J Geol. 2024;14(2):196–246.
Koçyiğit A. An overview on the main stratigraphic and structural features of a geothermal area: the case of Nazilli-Buharkent section of the Büyük Menderes Graben, SW Türkiye. Geodinam Acta. 2015;27(2–3):85–109. https://doi.org/10.1080/09853111.2014.957501.
Liotta D, Brogi A, Ruggieri G, Rimondi V, Zucchi M, Helgadóttir HM, et al. Fracture analysis, hydrothermal mineralization and fluid pathways in the Neogene Geitafell central volcano: insights for the Krafla active geothermal system, Iceland. J Volcanol Geotherm Res. 2020;391:106502. https://doi.org/10.1016/j.jvolgeores.2018.11.023.
Liotta D, Brogi A, Árnadóttir S, Ágústsson K, Thorsteinsdóttir U. Field evidence of the interplay between rift and transform structures in the Krafla geothermal area, N-Iceland. Geothermics. 2021. https://doi.org/10.1016/j.geothermics.2020.102039.
Marchesini B, Pozzi G, Collettini C, Carminati E, Tesei T. Caprock genesis in hydrothermal systems via alteration-controlled fault weakening and impermeabilization. J Geophys Res: Solid Earth. 2025;130(2):e2024JB030565.
Meixner J, Schill E, Grimmer JC, Gaucher E, Kohl T, Klingler P. Structural control of geothermal reservoirs in extensional tectonic settings: an example from the Upper Rhine Graben. J Struct Geol. 2016;82:1–15. https://doi.org/10.1016/j.jsg.2015.11.003.

Moeck IS. Catalog of geothermal play types based on geologic controls. Renew Sustain Energy Rev. 2014;37:867–82. https://doi.org/10.1016/j.rser.2014.05.032.
Oberhänsli R, Candan O, Wilke FDH. Geochronological evidence of Pan-African eclogites from the Central Menderes Massif, Turkish Journal. Earth Sci. 2010;19:431–47.
Okay AI, İşintek İ, Altıner D, Özkan-Altıner S, Okay N. An olistostrome–mélange belt formed along a suture: Bornova Flysch zone, western Türkiye. Tectonophysics. 2012;568:282–95.
Özkaptan M, Gülyüz E, Uzel B, Langereis CG, Özacar AA, Kaymakcı N. Deformation in SW Anatolia (Türkiye) documented by anisotropy of magnetic susceptibility data. Tectonics. 2021;40(12):e2021TC006882.
Pérez-Flores P, Veloso E, Cembrano J, Sánchez-Alfaro P, Lizama M, Arancibia G. Fracture network, fluid pathways and paleostress at the Tolhuaca geothermal field. J Struct Geol. 2017;96:134–48. https://doi.org/10.1016/j.jsg.2017.01.009.
Philippon M, Brun JP, Gueydan F, Sokoutis D. The interaction between Aegean back-arc extension and Anatolia escape since middle Miocene. Tectonophysics. 2014;631:176–88.
Pichon XL, Angelier J. The Hellenic Arc and Trench system: a key to the neotectonic evolution of the eastern Mediterranean area. Tectonophysics. 1979;60(1–2):1–42. https://doi.org/10.1016/0040-1951(79)90131-8.
Ring U, Johnson C, Hetzel R, Gessner K. Tectonic denudation of a late Cretaceous-Tertiary collisional belt: Regionally symmetric cooling patterns and their relation to extensional faults in the Anatolide belt of western Türkiye. Geol Mag. 2003;140:421–41.
Roche V, Sternai P, Guillou-Frottier L, Menant A, Jolivet L, Bouchot V, et al. Emplacement of metamorphic core complexes and associated geothermal systems controlled by slab dynamics. Earth Planet Sci Lett. 2018;498:322–33. https://doi.org/10.1016/j.epsl.2018.06.043.
Roche V, Bouchot V, Beccaletto L, Jolivet L, Guillou-Frottier L, Tuduri J, et al. Structural, lithological, and geodynamic controls on geothermal activity in the Menderes geothermal Province (Western Anatolia, Türkiye). Int J Earth Sci. 2019;108:301–28. https://doi.org/10.1007/s00531-018-1655-1.
Şalk M, Pamukçu O, Kaftan I. Determination of the curie point depth and heat flow from Magsat data of Western Anatolia. J Balk Geophys Soc. 2005;8:149–60.
Sarıca N. The Plio-Pleistocene age of Büyük Menderes and Gediz grabens and their tectonic significance on N-S extensional tectonics in West Anatolia: mammalian evidence from the continental deposits. Geol J. 2000;35:1–24. https://doi.org/10.1002/(SICI)1099-1034(200001/03)35:13.3.CO;2-1.
Şengör AMC. Cross-faults and differential stretching of hanging walls in regions of low-angle normal faulting: examples from western Türkiye. Geol Soc. 1987;28(1):575–89. https://doi.org/10.1144/gsl.sp.1987.028.01.38.
Şengör AMC, Satir M, Akkök R. Timing of tectonic events in the Menderes Massif, western Türkiye: implications for tectonic evolution and evidence for pan-African basement in Türkiye. Tectonics. 1984;3(7):693–707. https://doi.org/10.1029/tc003i007p00693.
Şengör, A. M. C., Görür, N., & Şaroğlu, F. (1985). Strike-slip faulting and related basin formation in zones of tectonic escape: Türkiye as a case study. Strike-Slip Deformation, Basin Formation, and Sedimentation, 227–264. https://doi.org/10.2110/pec.85.37.0227.
Siefert D, Wolfgramm M, Kölbel T, Glodny J, Kolb J, Eiche E. Geothermal reservoir rocks of the Büyük Menderes Graben (Türkiye): stratigraphic correlation by a multiproxy approach. Turk J Earth Sci. 2021;30:1008–31. https://doi.org/10.3906/yer-2104-11.
Şimşek Ş. Geothermal model of Denizli, Sarayköy-Buldan area. Geothermics. 1985;14(2–3):393–417.
Simsek S. Hydrogeological and isotopic survey of geothermal fields in the Buyuk Menderes graben, Türkiye. Geothermics. 2003;32(4–6):669–78.
Şimşek, Ş., (1984). Denizli-Kızıldere-Tekkehamam-Tosunlar-Buldan-Yenice alanının jeolojisi ve jeotermal enerji olanakları. Mineral Res. Expl. Direct. Türkiye (MTA), Scientific Report No: 7846, p. 85. Ankara, Türkiye (in Turkish).
Sümer Ö, Sözbilir H, Uzel B. Büyük Menderes Grabeni'nin Rolling Hinge (Yuvarlanan Reze) Modelinde Supra-Detachment (Sıyrılma Üstü) Havzadan Rift Havzasına Evrimi. Türkiye Jeoloji Bülteni 2020;63(3):241-276
TEİAŞ (2020). Türkiye Elektrik İletim Anonim Şirketi Türkiye Elektrik İletim A.Ş. Kurulu Güç Raporu, Aralık 2020 (in Turkish).https://www.teias.gov.tr/faaliyet-raporlari
Ten Veen JH, Boulton SJ, Alçiçek MC. From palaeotectonics to neotectonics in the Neotethys realm: the importance of kinematic decoupling and inherited structural grain in SW Anatolia (Türkiye). Tectonophysics. 2009;473:261–81.
Tezel T, Shibutani T, Kaypak B. Crustal thickness of Türkiye determined by receiver function. J Asian Earth Sci. 2013;75:36–45.
Thomson SN, Ring U. Thermochronologic evaluation of postcollision extension in the Anatolide orogen, western Türkiye. Tectonics. 2006. https://doi.org/10.1029/2005TC001833.
Uzel B, Sözbilir H, Özkaymak Ç, Kaymakçı N, Langeris CG. Structural evidence for strike-slip deformation in the İzmir-Balıkesir transfer zone and consequences for late Cenozoic evolution of western Anatolia (Türkiye). J Geodyn. 2013;65:94–116. https://doi.org/10.1016/j.jog.2012.06.009.
Uzel B, Kuiper K, Sözbilir H, Kaymakci N, Langereis CG, Boehm K. Miocene geochronology and stratigraphy of western Anatolia: insights from new Ar/Ar dataset. Lithos. 2020;352:105305.
Van der Pluijm BA, Marshak S. Earth structure: an introduction to structural geology and tectonics. 2nd ed. New York: W. W. Norton & Company, Inc.; 2004.
van Heiningen PS, Kaymakci N. Neogene drainage evolution of SW Anatolia (Türkiye): integration of morphotectonics, drainage and denudation analyses. Earth Surf Process Landforms. 2024;49(15):5284–308.
Vanacore EA, Taymaz T, Saygin E. Moho structure of the Anatolian Plate from receiver function analysis. Geophys J Int. 2013;193(1):329–37.
Westaway R. Present-day kinematics of the Middle East and eastern Mediterranean. J Geophys Res: Solid Earth. 1994;99(B6):12071–90. https://doi.org/10.1029/94jb00335.

Publisher's Note

Springer Nature remains neutral with regard to jurisdictional claims in published maps and institutional affiliations.